The Electrochemical Society
Advancing solid state & electrochemical science & technology

Review—Influence of Processing Parameters to Control Morphology and Optical Properties of Sol-Gel Synthesized ZnO Nanoparticles

View the article online for updates and enhancements.

The Electrochemical Society
Advancing solid state & electrochemical science & technology

242nd ECS Meeting

Oct 9 – 13, 2022 • Atlanta, GA, US

Abstract submission deadline: **April 8, 2022**

Connect. Engage. Champion. Empower. Accelerate.

MOVE SCIENCE FORWARD

Submit your abstract

Review—Influence of Processing Parameters to Control Morphology and Optical Properties of Sol-Gel Synthesized ZnO Nanoparticles

Sandeep Arya,[1,z] Prerna Mahajan,[1] Sarika Mahajan,[2] Ajit Khosla,[3] Ram Datt,[4] Vinay Gupta,[5] Sheng-Joue Young,[6] and Sai Kiran Oruganti[7]

[1]*Department of Physics, University of Jammu, Jammu and Kashmir 180006, India*
[2]*Department of Electronics, Government M. A. M. College Jammu, Jammu and Kashmir 180006, India*
[3]*Department of Mechanical System Science, Graduate School of Science and Engineering, Yamagata University, Yonezawa, Yamagata 992-8510, Japan*
[4]*SPECIFIC, College of Engineering, Bay Campus, Swansea University, Swansea- SA1 8EN, United Kingdom*
[5]*Department of Mechanical Engineering, Khalifa University of Science and Technology, Masdar campus, Abu Dhabi 54224, UAE*
[6]*Department of Electronic Engineering, National Formosa University, Yunlin 632, Taiwan*
[7]*Department of Electrical Engineering, Jiangxi university of Science and Technology, Ganzhou 341000, People's Republic of China*

ZnO has several potential applications into its credit. This review article focuses on the influence of processing parameters involved during the synthesis of ZnO nanoparticles by sol-gel method. During the sol-gel synthesis technique, the processing parameters/ experimental conditions can affect the properties of the synthesized material. Processing parameters are the operating conditions that are to be kept under consideration during the synthesis process of nanoparticles so that various properties exhibited by the resulting nanoparticles can be tailored according to the desired applications. Effect of parameters like pH of the sol, additives used (like capping agent, surfactant), the effect of annealing temperature and calcination on the morphology and the optical properties of ZnO nanoparticles prepared via sol-gel technique is analyzed in this study. In this study, we tried to brief the experimental investigations done by various researchers to analyze the influence of processing parameters on ZnO nanoparticles. This study will provide a platform to understand and establish a correlation between the experimental conditions and properties of ZnO nanoparticles prepared through sol-gel route which will be helpful in meeting the desired needs in various application areas.

Zinc oxide (ZnO) acts as a multifunctional material because of its remarkable and distinctive physical as well as chemical properties, for instance, high chemical stability, high electrochemical coupling coefficient, high photostability, a broad radiation absorption range, etc.[1,2] ZnO is a direct band gap semiconductor that belongs to group II–VI. It has a wide band gap of 3.37 eV and possesses high exciton binding energy of 60 meV.[3] ZnO exhibits unique optical, electronic as well as magnetic properties that are different from its bulk counterpart.[4] It offers applications in a variety of devices like field emission devices, electroluminescent devices, optoelectronic and electronic devices.[5–8] ZnO possesses outstanding characteristics for example easy preparation procedure, tunable band gap, low production cost, convenient shape and size, etc.[9] ZnO offers piezoelectric and pyroelectric properties that make it apposite for utilization as a sensor, photocatalyst, energy generator and convertor.[10,11] Due to its stability, rigidity and piezoelectric constant it has also become a significant matter in the ceramic industry. ZnO is a less-toxic, biodegradable and biocompatible material which makes it suitable for use in the biomedicinal and pro-ecological area.[12–14] It offers vast applications in drug delivery and bioimaging systems. It is also used in antidiabetic, anticancer, antioxidant, antibacterial and anti-inflammatory activities.[15,16] ZnO offers promising utilization in cosmetic products like sunscreen attributing to its strong UV absorption properties, good antifouling and antibacterial properties.[17,18]

ZnO offers an assorted range of morphologies viz. nanorods,[19–21] nanorings,[22] nanowires,[23,24] nanobelts,[25] nanocages,[26] nanocombs[27] etc. As reviewed from literature, a variety of techniques have been adopted for the growth of ZnO nanostructures like electrochemical deposition method,[28] chemical vapor deposition method,[29] sol-gel method,[30] pulsed laser deposition,[31] hydrothermal method,[32] thermal decomposition,[33] microwave assisted technique,[34] spray pyrolysis,[35,36] co-precipitation,[37] sputtering[38] and solvothermal method.[39]

In this review article, we present a study on the influence of various processing parameters (sometimes called as reaction conditions or experimental conditions) on ZnO nanoparticles prepared via sol-gel synthesis technique. By selectively controlling the size and shape of ZnO nanostructures, this field is gaining importance and is becoming a field of interest because of the number of size and shape-dependent applications that these ZnO nanostructures offer.[40] The size and morphology of the nanoparticles influences their optical properties and the morphology can be effectively controlled through the hydrolysis and condensation reactions that take place during the sol-gel synthesis.[41,42] Therefore, with the aim of tailoring the properties of nanoparticles according to a specific application, it becomes necessary to understand the dependence relationship of the physical/chemical properties of the synthesized nanoparticles; and the operating conditions during their sol-gel synthesis process.

Potentials of the Sol-Gel Process

Sol-gel technique is being considered very advantageous for synthesizing materials owing to its effortlessness, reproducibility, consistency and economical nature. The sol-gel synthesized nanoparticles offer good optical properties.[43] The sol-gel process can be employed to synthesize different forms of materials such as nanoparticles, thin-film coatings, ceramics; offering a wide variety of applications.[44]

In this method, an inorganic network is synthesized through a chemical reaction that is being produced in the solution at low temperature.[45] The sol-gel method offers a number of merits like excellent homogeneity and purity of synthesized product; it has been found to be economical and convenient. It is used to synthesize high-quality homogenous nanoparticles using non-vacuum conditions.[46]
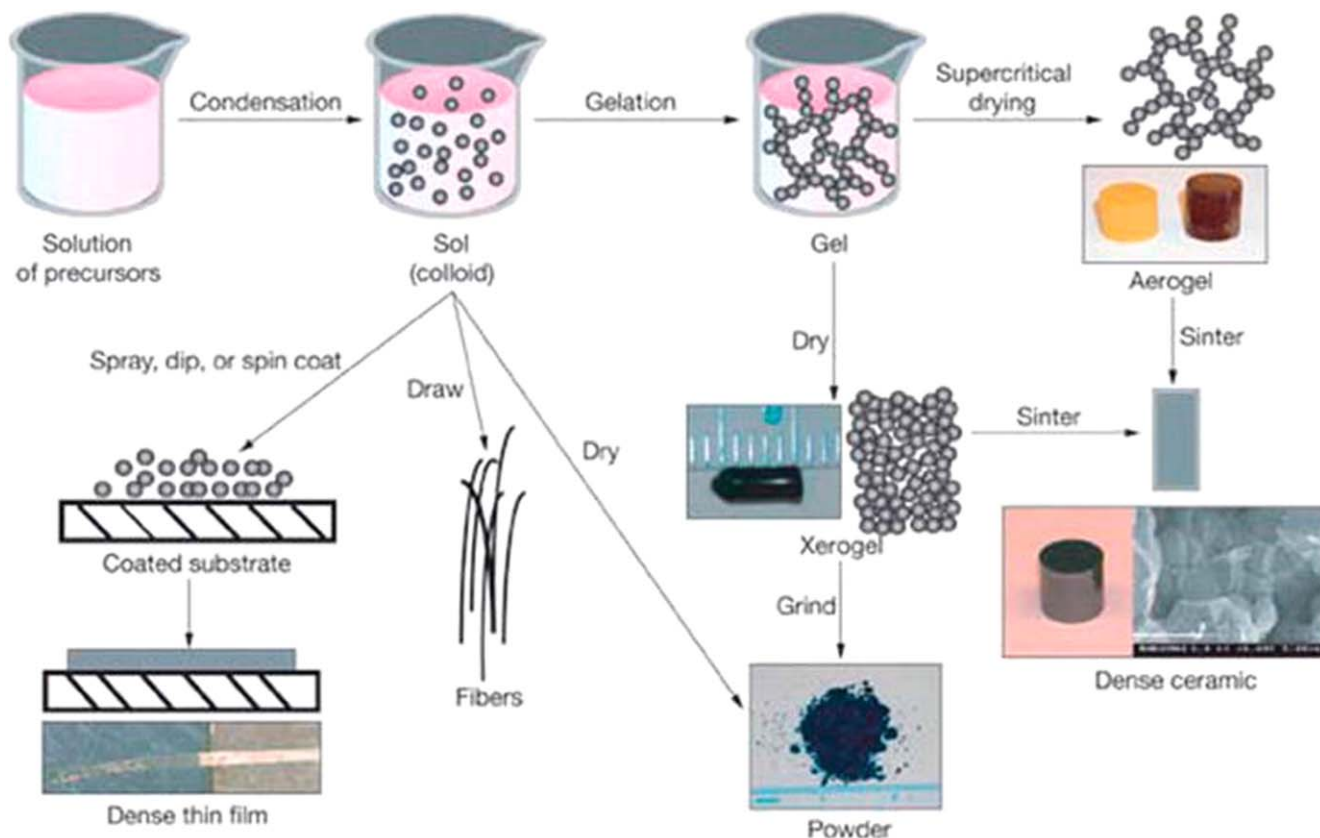
Figure 1. Processing stages involved in the sol-gel method. Reproduced from Ref. 48 under Creative Commons Attribution 3.0 license, Copyright@2018, IntechOpen.

In sol-gel technique, hydrolysis and condensation reactions are involved in an organometallic precursor (like alkoxides, chloride, beta-diketonate or nitrate) under aqueous conditions forming a solid material. In the beginning, the precursor solution undergoes hydrolysis and condensation reactions leading to the formation of gel; which is followed by ageing, solvent extraction and drying treatment of synthesized product so as to get the required material.[47] Figure 1 describes the schematic procedure of synthesizing nanomaterials via sol-gel preparation technique.[48]

Sol-gel is a trouble-free and convenient technique that offers the ability to synthesize ZnO nanoparticles exhibiting controlled morphology and size.[49] The sol-gel method is a conventional method employed for synthesizing metal oxides in a variety of forms such as xerogels, aerogels, fibres, thin films, nanoparticles, microparticles, etc. This method of synthesis produces homogenous and porous oxides at low processing temperature. The synthesized materials are achieved in different forms. These resulting materials obtained from the sol-gel method of synthesis are applied in a number of applications like protective coatings, heterogeneous catalysts, optoelectronic materials and many more.[50–53] This process offers control over the physico-chemical properties of resulting compounds by careful variation in processing parameters during synthesis.[54] The various parameters that could affect the synthesized material and could be selectively controlled are nature of precursor, type of solvent used, the molar ratio of reactants, pH of the solution, type and concentration of additives used (catalysts, surfactants, capping agent), ageing period, pre and post-heat treatment.[45,54,55]

Sol-Gel Synthesis of ZnO Nanoparticles

ZnO is a white to yellowish-white crystalline powder in appearance. It is nearly soluble in water.[56] There are three crystallization forms of ZnO viz. cubic zinc blende, hexagonal wurtzite, and cubic rocksalt. Out of these forms, the cubic rocksalt structure is
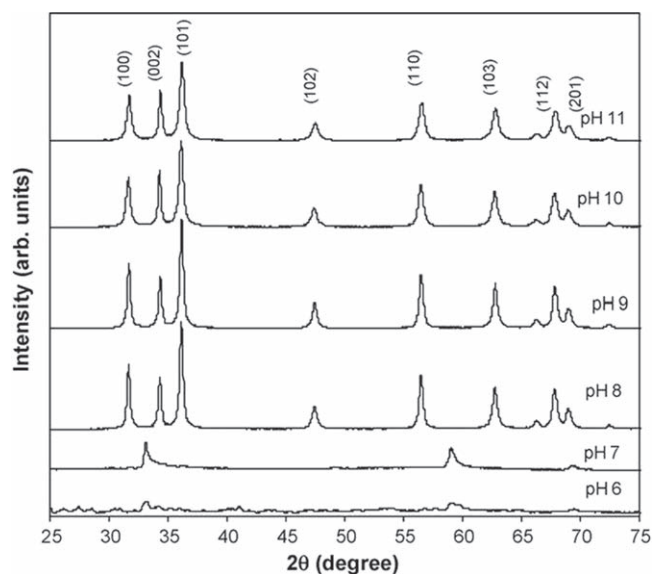

Figure 2. XRD results of ZnO nanoparticles synthesized at different pH values (pH 6–11). Reproduced from Ref. 68 with permission, Copyright@2010, Elsevier.

rarely observed while the hexagonal wurtzite crystal structure is the most stable at room temperature.[57] ZnO is a polar crystal having octahedral geometry. Here, Zn and O atoms are alternatively arranged along the *c*-axis direction with hexagonal phase. The synthesis technique utilized and the processing conditions robustly affect the properties of ZnO. Further, the growth mechanism of ZnO depends on various external conditions such as solution pH, reaction
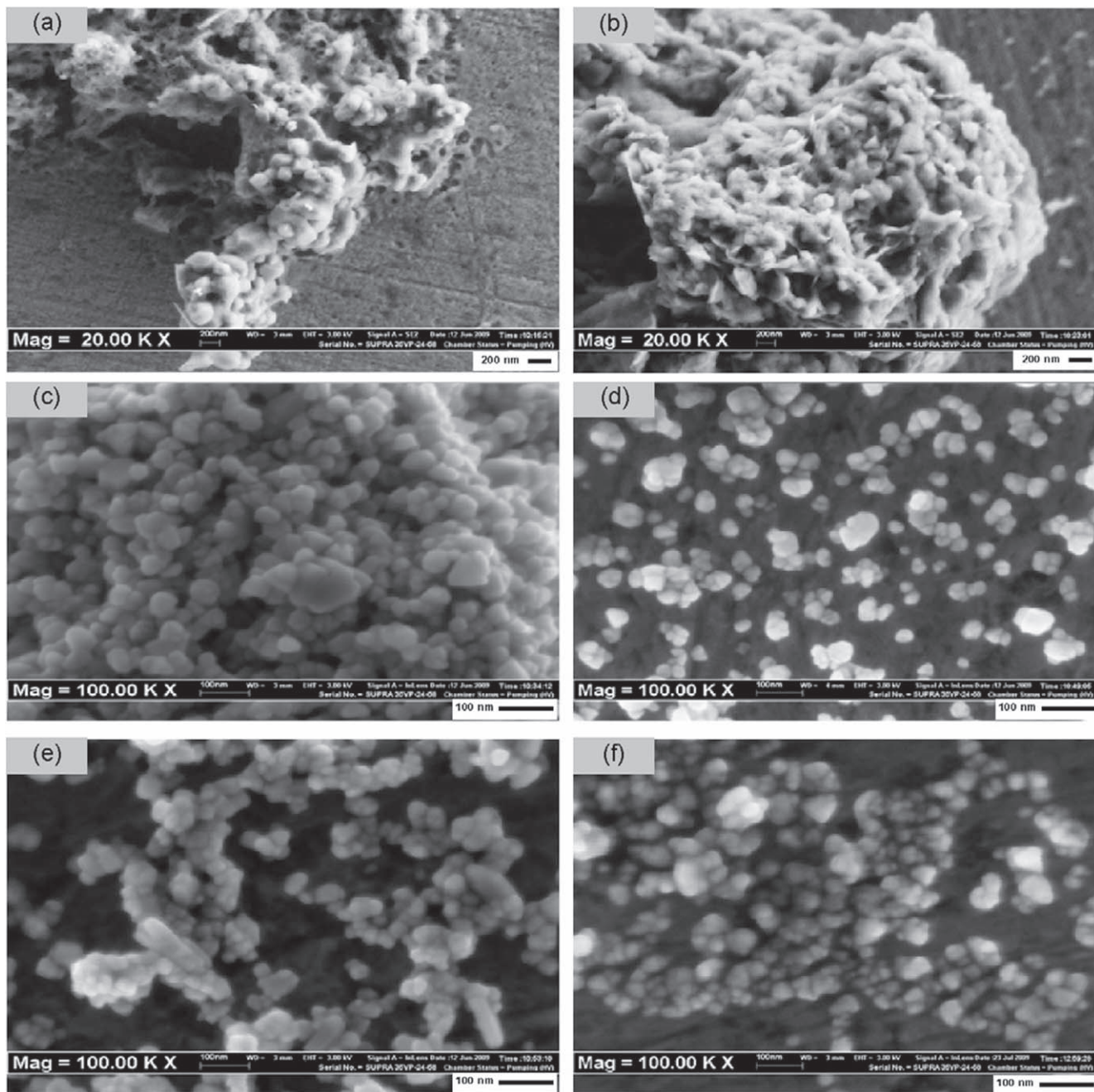
Figure 3. FESEM of different samples of ZnO nanoparticles at (a) pH 6, (b) pH 7, (c) pH 8, (d) pH 9, (e) pH 10 and (f) pH 11. Reproduced from Ref. 68 with permission, Copyright@2010, Elsevier.

concentration and temperature.[58–60] ZnO offers excellent mechanical, electrical and optical properties.[61] At nanoscale due to reduction in size, ZnO nanoparticles shows a variation in physical properties, hence results in better and improved properties in comparison to the properties offered by bulk ZnO.[62] Formation of polymeric hydroxides is the basic requirement of sol-gel technique and Zn belongs to that group of elements which can easily form polymeric hydroxides.[46] So, the sol-gel method is very useful for the synthesis of ZnO in the form of nanoparticles or thin films. Further, this method is utilized on account of its less processing cost, easiness and good control over particle size.[63] The diverse properties offered by ZnO are believed to be dependent on the variety of morphologies exhibited by ZnO.[64] The sol-gel method is an attractive process as it offers various advantages like simplicity, high reliability, low processing temperature, good repeatability, less production cost in

comparison to other synthesis processes and excellent compositional homogeneity. It also provides effective control of the morphology, optical properties and physical characteristics of the synthesized nanoparticles.[43,65]

In this review paper, we have tried to summarize the experimental investigations conducted by researchers to analyze the influence of various processing factors like pH, calcinations/annealing temperature and capping agents, on morphological and optical properties of sol-gel synthesized ZnO nanoparticles.

Influence of pH.—The morphology of the sol-gel synthesized metal oxide nanoparticles strongly depends on the amount of H^+ or OH^- ions present in the sol. These ions determine the metal-oxygen bond polymerization during the ZnO growth process. The hydrolysis and condensation reactions occurring in the precursor solution
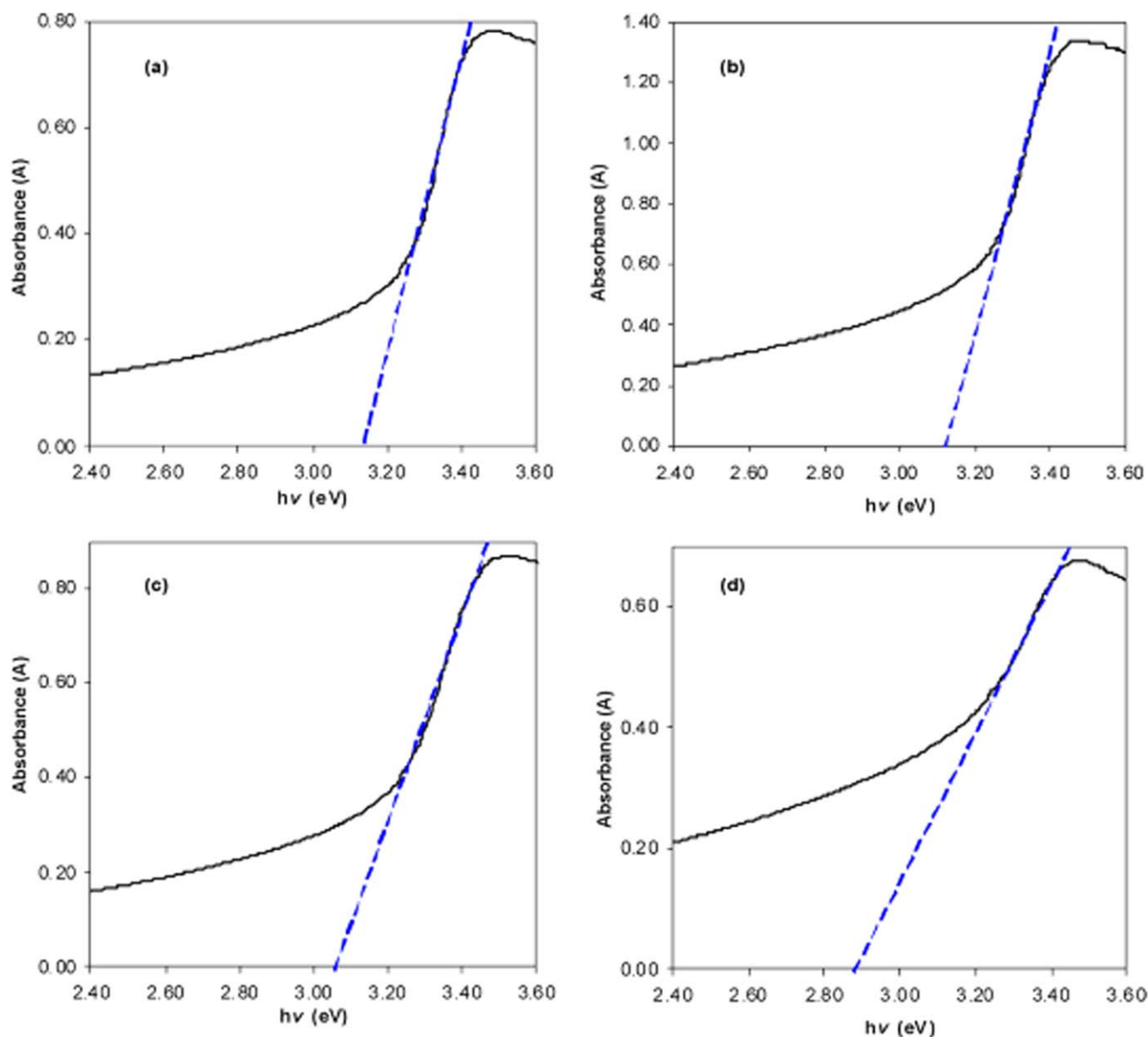
Figure 4. UV–vis analysis plot for ZnO at (a) pH 8, (b) pH 9, (c) pH 10 and (d) pH 11. Reproduced from Ref. 68 with permission, Copyright@2010, Elsevier.

Table I. Variation in particle size, crystallite size and band gap energy of the synthesized ZnO nanoparticles at various pH values. Reproduced from Ref. 68 with permission, Copyright@2010, Elsevier.

pH value	8	9	10	11	Observations
Particle size (nm)	49.98	48.31	38.32	36.65	Decrease in particle size with increase in pH was observed.
Crystallite size (nm)	24.96	25.36	21.87	18.37	Decrease in crystallite size with increase in pH was observed.
Energy gap E_g (eV)	3.25	3.24	3.23	3.14	Decrease in band gap energy with increase in pH was observed.

during gel formation is affected by the variation in pH value of the solution. This distinction in pH further influences the morphology of synthesized particles.[66] A variation in the pH of the solution can also lead to the variation in the number of ZnO nuclei and growth units.[67] So it becomes necessary to establish the relation between size variation of nanoparticles and processing parameters or experimental conditions so as to tailor/tune the required properties of the nanomaterials according to the desired applications.

In a study, S.S. Alias et al.[68] examined the consequence of variation in pH of the sol on the properties of ZnO nanoparticles

prepared by the sol-gel process. Zinc acetate dihydrate (Zn(CH$_3$COO)$_2$.2H$_2$O), methanol (CH$_3$OH) and sodium hydroxide (NaOH) were used for synthesis. Sodium hydroxide was used to manage the pH of the solution. Different samples were prepared for analysis by varying the pH values of solutions from 6 (acidic) to 11 (alkaline). Figure 2 shows the XRD results of the synthesized nanoparticles and it confirms the formation of ZnO in its hexagonal wurtzite structure.

There was no peak of ZnO in the XRD graph at pH 6 and 7. This shows that, at pH 6, ZnO nanostructure could not be synthesized
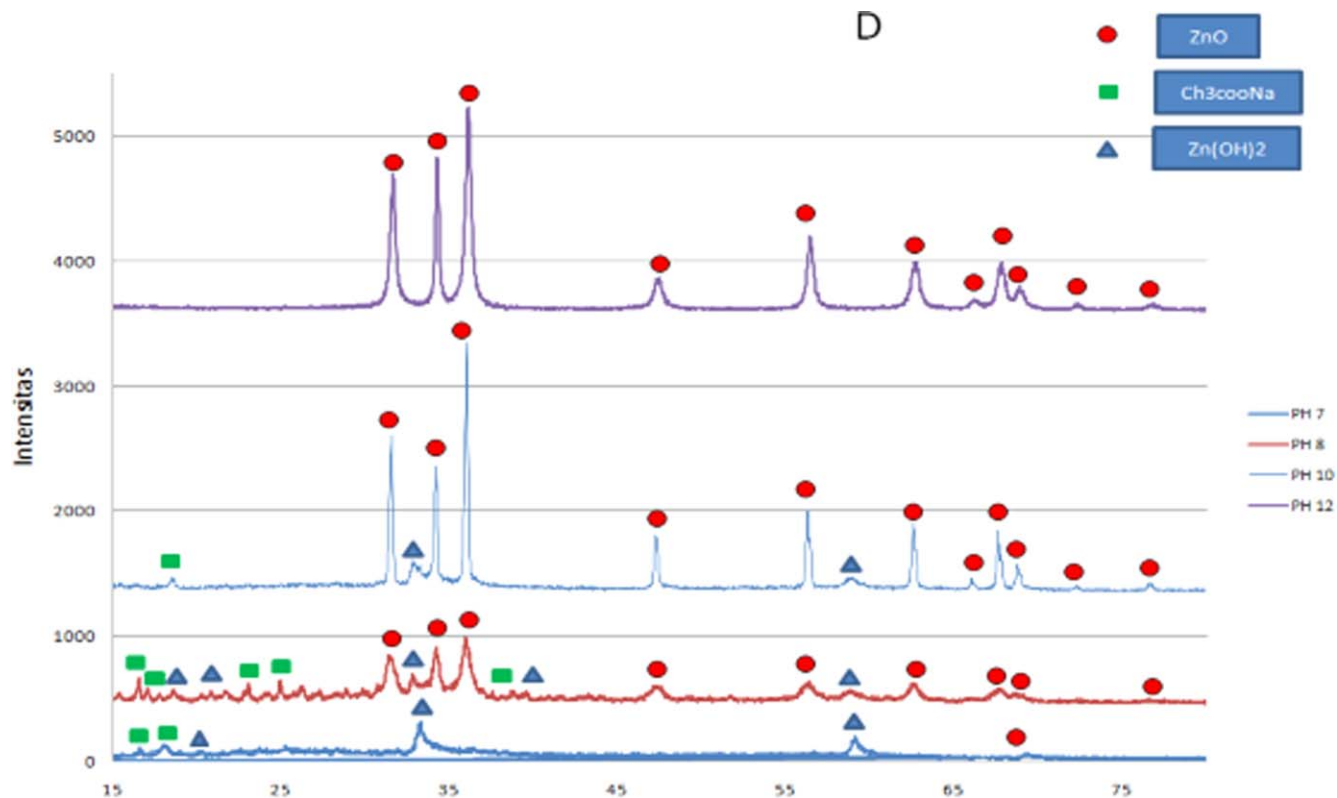
Figure 5. XRD results of the synthesized sample at pH 7, 8, 10 and 12. Reproduced from Ref. 69 under Creative Commons Attribution 3.0 license, Copyright@2017, IOP Science.

Table II. Effects of pH on the size of the crystal and percentage of ZnO. Reproduced from Ref. 69 under Creative Commons Attribution 3.0 license, Copyright@2017, IOP Science.

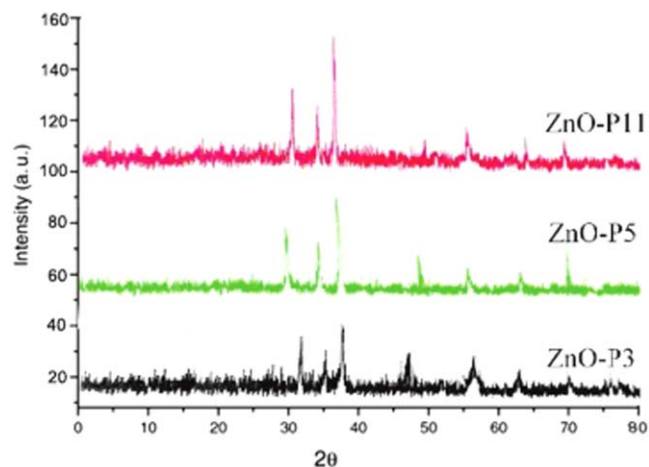| pH	crystallite size (nm)	% of ZnO
7	10.94 ± 0.99 nm	42.9
8	17.44 ± 5.36 nm	62.2
10	38.27 ± 2.14 nm	64.7
12	74.04 ± 41.77 nm	100

Figure 6. XRD of the ZnO samples (pH-3,5,11) annealed at 600 °C. Reproduced from Ref. 70 with permission, Copyright@2016, AIP Publishing.

since, at this pH, the system is acidic and as a result, H^+ ions are present in high concentration and OH^- ions are present in less concentration in the solution. However, at pH 7, the solution is neutral since there is an equal concentration of H^+ ions and OH^- ions in the system. For the pH values of 8–11, the graph shows significant peaks corresponding to ZnO wurtzite structure. At pH values of 6 and 7, large and bulk agglomerated particles were observed in FESEM images as shown in Figs. 3a, 3b. This agglomeration was a consequence of insufficient OH^- ions in $Zn(OH)_2$ sols attributed to their acidic (pH 6) and neutral (pH 7) pHs. It was further mentioned that at pH 8 and pH 9, the particles were homogenous, having good nanostructures (Figs. 3c, 3d). ZnO nanoparticles were observed to be spherical in shape. Above pH 9, the particle size of the nanoparticles was found to decrease with an increase in pH value of the sols (Figs. 3e, 3f). The crystallite size of the synthesized ZnO nanoparticles was found in the range 18.37 nm to 25.36 nm. At pH 9, the largest crystallite size was observed while at pH 11, the smallest crystallite size occurred. On the other hand, the particle size was found to be in the range 36.65 nm to 49.98 nm. Both the crystallite size and particle size have shown a decreasing trend with the increasing pH. Thus, this study concluded that crystallite size and particle size of synthesized ZnO nanoparticles are inversely proportional to their pH values.

While analyzing the optical properties, it was observed that for pH 6 and pH 7, the band gap energy values (E_g) were not shown due to agglomerated and large particle size. Figures 4a–4d shows the UV–vis analysis plot for ZnO at pH 8–11. It was further mentioned that the particle size strongly influences the level of optical absorption. The band gap energy was observed to decrease with a decrease in particle size whereas the particle size was found to decrease with an increase in pH. Table I shows the variation in particle size, crystallite size and band gap energy of the synthesized ZnO nanoparticles at pH 8–11.
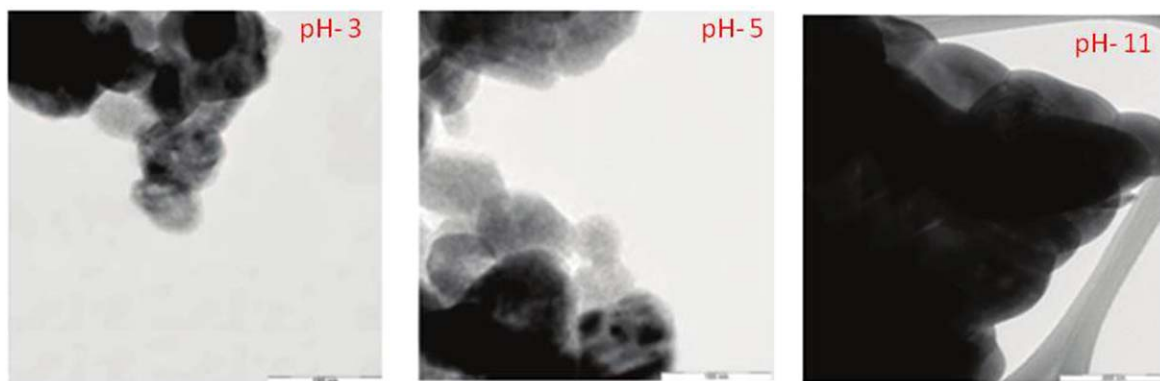
Figure 7. TEM images of the synthesized samples of ZnO at different pH values (pH-3,5,11). Reproduced from Ref. 70 with permission, Copyright@2016, AIP Publishing.
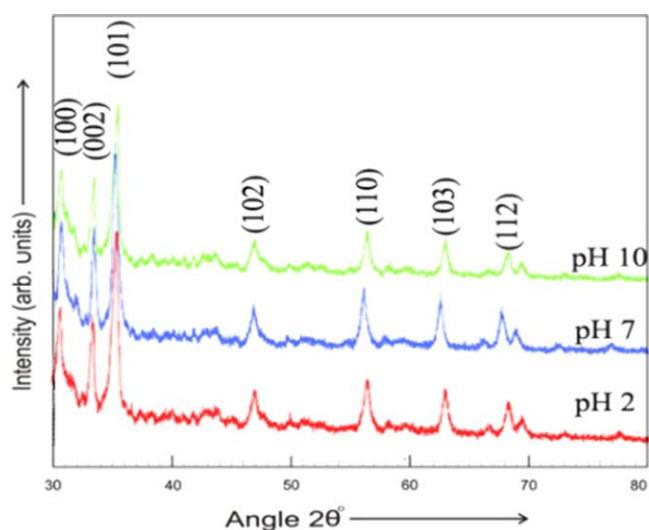

Figure 8. XRD patterns of the synthesized ZnO at different pH values (pH-2,7,10). Reproduced from Ref. 71 with permission, Copyright@2015, Elsevier.

In another investigation, Siswanto et al.[69] examined the consequence of variation in pH of the solution on the size of sol-gel synthesized ZnO nanoparticles. In this study, zinc acetate dihydrate, sodium hydroxide, methanol and aquabidest were employed to synthesize ZnO. Different samples of colloidal solution were prepared with variation in pH value (pH 7, 8, 9, 10, 11, 12). From the XRD observations (Fig. 5) it was found that at pH 7 and 8, ZnO was not completely formed. The formation of ZnO began at pH 10, and at pH 12 the formation of pure ZnO nanoparticles occurred. It was found that at pH 7, the average particle size obtained was 1.3 nm while it was 73.8 nm at pH 12.

From the obtained crystal sizes, it was observed that larger was the pH value, larger was the crystal size and for smaller pH value, smaller was the crystal size. It was mentioned that the sample synthesized at pH 12 has particle size 73.8 nm and composition of 100% ZnO. Table II shows the pH effect on the size of the crystal and the percentage of ZnO.

K. Lee et al.[70] also investigated the effect of pH on the size of sol-gel synthesized ZnO nanoparticles. Here, zinc acetate and citric acid were utilized for synthesis purpose. Further, for adjusting the pH of the solution, sodium hydroxide was employed. Three samples were prepared with pH 3.0, pH 5.0 and pH 11.0. Figure 6 shows the XRD graph of the prepared ZnO which shows the complete formation of ZnO at 600 °C in its hexagonal phase. TEM results are shown in Fig. 7 and these images were utilized to estimate the size of the samples. The average size of the ZnO nanoparticles was found around 70 nm for pH 3, 100 nm for pH 5 and 200 nm for pH 11. It was observed that with an increase in the pH of the precursor, there was an increase in the particle size. Thus, the smaller size of the particle could be obtained at smaller pH value of precursor.
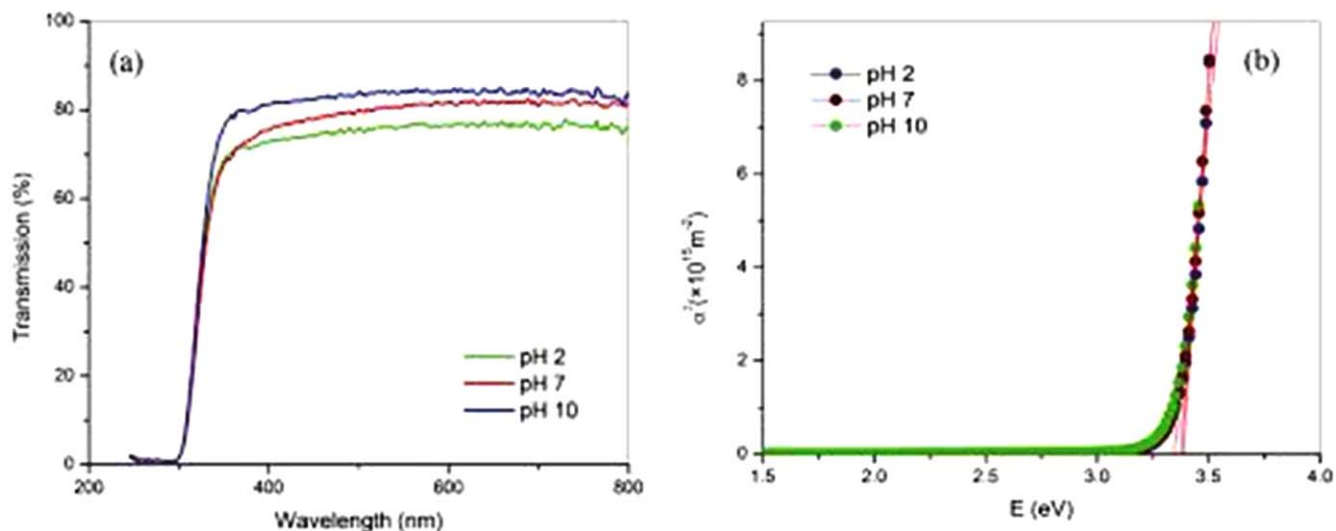

Figure 9. Variation of (a) Transmission plot, (b) Optical band gap energy of the synthesized samples of ZnO with the change in pH. Reproduced from Ref. 71 with permission, Copyright@2015, Elsevier.
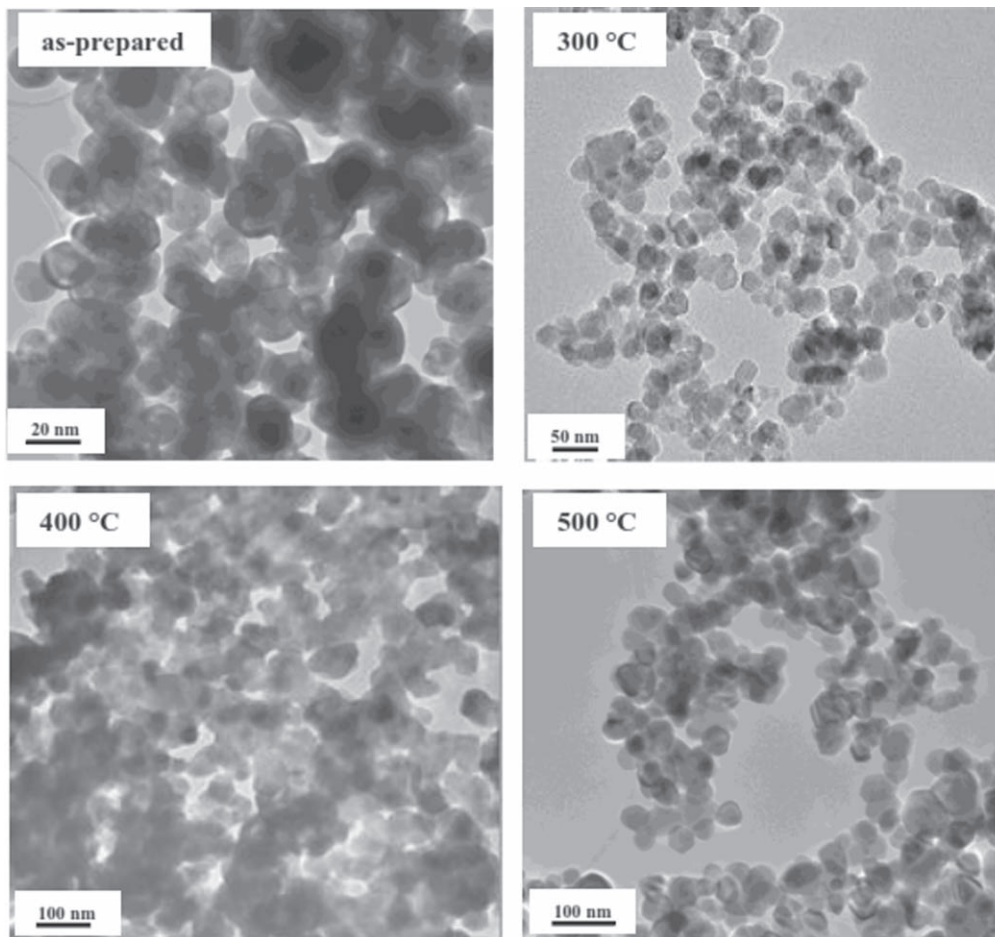
Figure 10. TEM images showing the morphology of ZnO nanopowder at various annealing temperatures. Reproduced from Ref. 77 with permission, Copyright@2014, Elsevier.

Similarly, R. Ashraf et al.[71] also investigated how the pH affects the structural and optical properties of sol-gel synthesized ZnO nanoparticles. The precursor employed was zinc acetate dihydrate and different solvents were taken to make the solution viz. deionized water (DI water), triethylamine and isopropyl alcohol (IPA). For controlling the pH, sodium hydroxide was utilized. Different samples were prepared for characterization at three different pH values of sol pH 2, pH 7 and pH 10. The XRD graph as shown in Fig. 8 confirmed the formation of ZnO nanoparticles with the wurtzite crystal structure. The crystallite sizes were determined that were found to decrease with the increasing pH value. At pH 2, a crystallite size of 23 nm (largest) was obtained while the smallest crystallite size (19 nm) was obtained at pH 10.

It was further observed that the prepared nanoparticles exhibited high transmittance from visible to IR region (Fig. 9a). Highest transmittance of 84% was exhibited by the sample synthesized at pH 10 which indicated that the transmittance of the synthesized ZnO nanoparticles increased with an increase in pH value. Further, the band gap as shown in Fig. 9b was also found to increase with the increasing pH from 3.34 eV to 3.38 eV and this increase in band gap energy was attributed to quantum confinement effect.[72]

Influence of calcination/annealing temperature.—ZnO is metal oxide semiconductor. The natural defects present in ZnO are zinc interstitial (Zn_i), zinc vacancy (V_{zn}), oxygen interstitial (O_i) and oxygen vacancy (V_o). Post-treatment annealing, accumulation of particular dopant and suitable growth temperatures are believed to control and remove the defects.[73–75] Hence, it is possible to tailor the properties of ZnO according to the required application.[76]
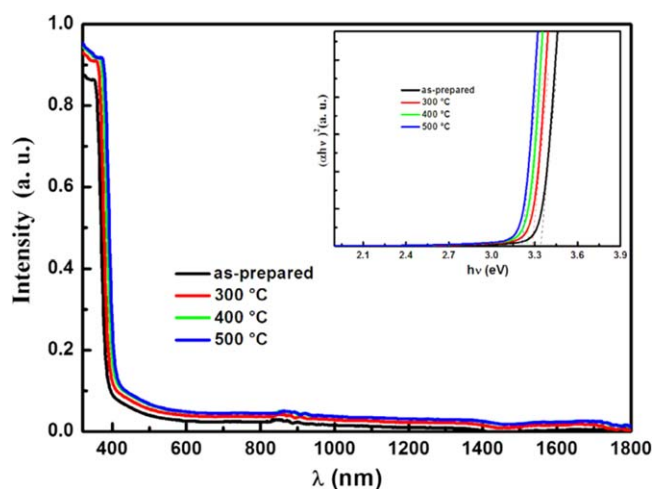
Figure 11. UV–vis-IR absorption spectrum and E_g spectrum (inset) of the synthesized samples at various annealing temperatures. Reproduced from Ref. 77 with permission, Copyright@2014, Elsevier.

In a study, K. Omri et al.[77] synthesized ZnO nanoparticles using zinc acetate dihydrate and methanol through the sol-gel process under supercritical drying of ethyl alcohol. Hexagonal wurtzite structure was observed from the results of XRD data. The prepared samples were subjected to annealing at several temperatures in air. The average grain size was found to increase from 33 nm to 52 nm

Table III. Variation in grain size with the annealing temperature. Reproduced from Ref. 77 with permission, Copyright@2014, Elsevier.

Annealing temperature (°C)	As-prepared	300	400	500
Grain size from Scherrer method (nm)	31.8	37.6	41.2	52.4
Grain size from TEM image (nm)	29–33	35–40	41–45	48–55
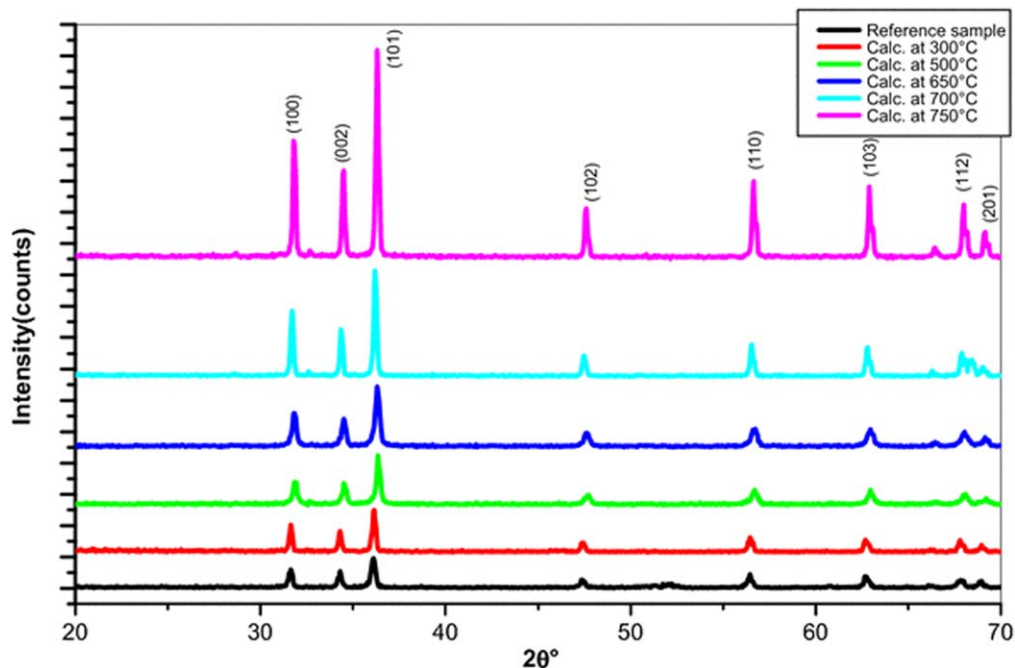
Figure 12. XRD graph of the reference (as- prepared) and calcined samples of ZnO nanoparticles at different temperatures. Reproduced from Ref. 78 with permission, Copyright@2015, Springer.
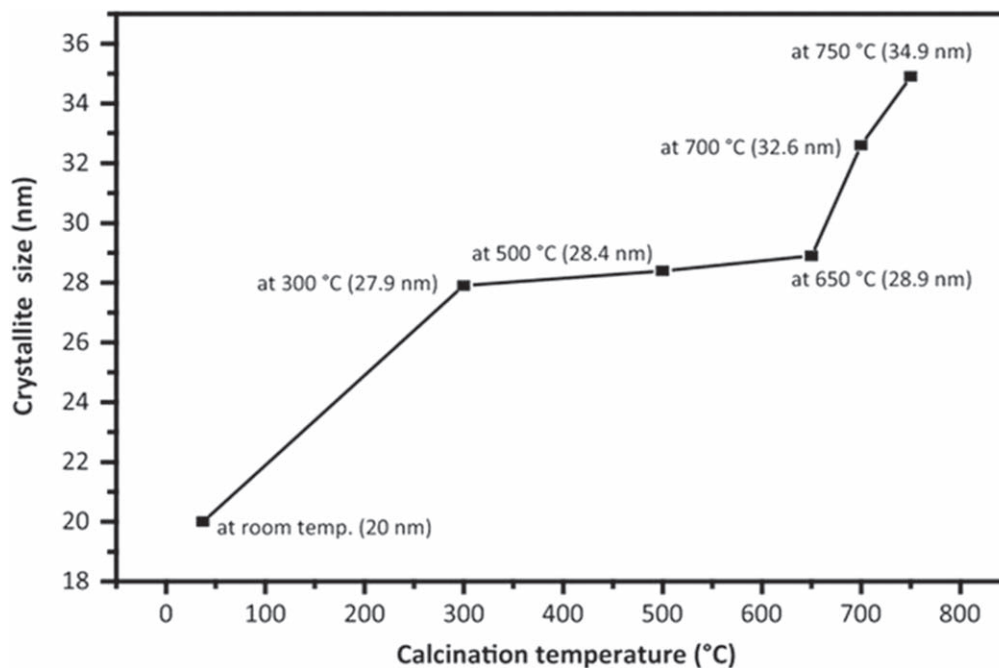
Figure 13. Variation in crystallite size obtained using the Scherrer method with the variation in calcination temperature. Reproduced from Ref. 78 with permission, Copyright@2015, Springer.

by increasing the annealing temperature, which was attributed to the merging process induced due to thermal annealing. TEM measurements (Fig. 10) showed that all the samples of nanoparticles exhibited nearly spherical shape with diameters in the range 38 nm to 54 nm. The grain size calculated from TEM images was also observed to increase with an increase in annealing temperature

Table IV. Variation in crystallite size, particle size and band gap energy with the change in calcination temperature. Reproduced from Ref. 78 with permission, Copyright@2015, Springer.

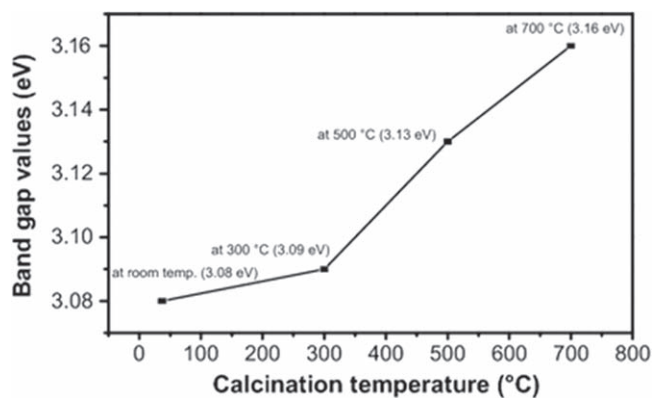| Calcination temperature	Room Temp.	300 °C	500 °C	650 °C	700 °C	750 °C	Variation with the increase in calcination temperature
Crystallite size (nm) D Scherrer method	20.0	27.9	28.4	28.9	32.6	34.9	Crystallite size increased
Particle size (nm)	27.9	31.4	45.8	48	54.3	—	Particle size increased
Band gap energy E_g (eV)	3.08	3.09	3.13	—	3.16	—	Band gap energy increased

Figure 14. Plot of band gap energy Vs calcination temperature. Reproduced from Ref. 78 with permission, Copyright@2015, Springer.
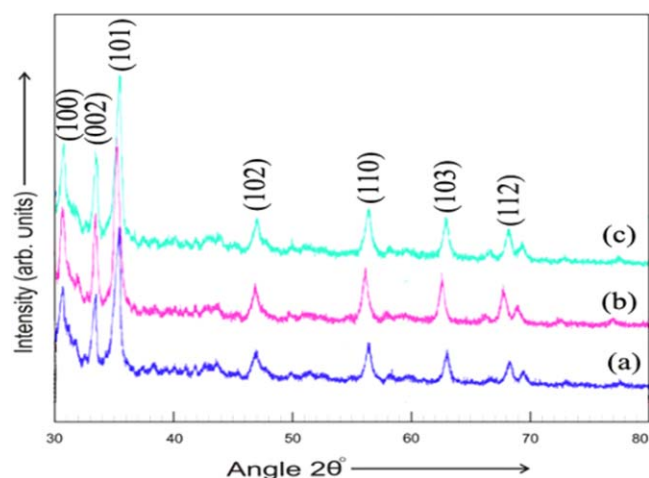

Figure 15. The XRD patterns of prepared samples of ZnO subjected to calcination at (a) 100 °C, (b) 200 °C and (c) 300 °C. Reproduced from Ref. 80 with permission, Copyright@2015, Elsevier.
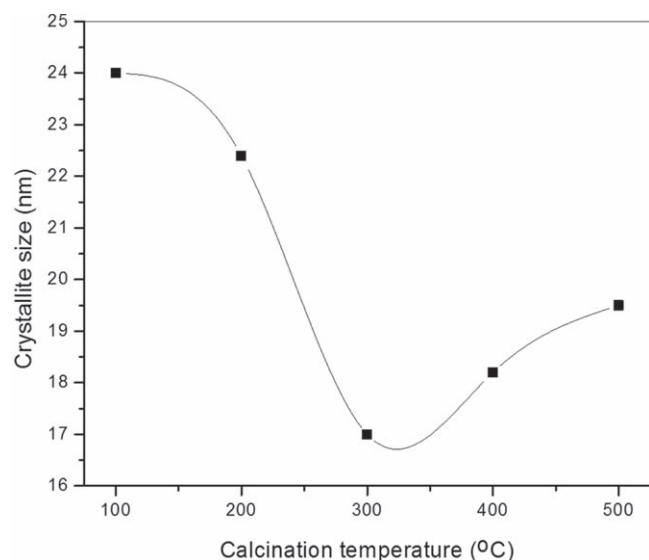

Figure 16. Plot of crystallite size obtained Vs calcination temperature. Reproduced from Ref. 80 with permission, Copyright@2015, Elsevier.

(Table III). The band gap energies were also determined at temperatures of 250 °C, 300 °C, 400 °C and 500 °C and were obtained as 3.34 eV, 3.28 eV, 3.24 eV, 3.21 eV respectively. So, it

was concluded that the band gap energy reduces with the enhancement in annealing temperature (Fig. 11).

Z. N. Kayani et al.[78] investigated the effect of calcination temperature on the structural and optical properties of sol-gel synthesized ZnO nanoparticles. Zinc acetate dihydrate and diethanolamine were utilized as precursors. Other reagents that were used are ethanol, ammonium hydroxide and distilled water. Different samples were obtained for characterization (as-prepared ZnO, samples calcined at 300 °C, 500 °C, 650 °C, 700 °C and 750 °C). Structural analysis was done by XRD (Fig. 12) which confirmed the presence of ZnO in its hexagonal wurtzite structure. As the sample was subjected to calcination from room temperature to 300 °C, the crystallite size sharply increased. On further increase in temperature from 300 °C–650 °C, crystallite size increased but very slightly. Thereafter, the sample showed an abrupt increase in crystallite size when the temperature was further increased to 750 °C (Fig. 13). Thus, we can conclude that the crystallite size of ZnO nanoparticles increases with the rise in calcination temperature. This was attributed to the coalescence of grains during calcination that in turn resulted in the merging of Zn or O defects at grain boundaries at high temperatures.[79] As the calcination temperature increased from 300 °C to 750 °C, the particle size also found to increase from 27.9 nm to 54.3 nm (Table IV).

The optical band gap energy was observed to be dependent on the calcination temperature. As the temperature increases from room temperature to 700 °C, the energy band gap also increased accordingly. The graph of change in optical band gap energy with the change in calcination temperature is shown in Fig. 14. The as-prepared ZnO nanoparticles exhibited band gap of 3.08 eV while the samples obtained after calcination at temperatures of 300 °C, 500 °C and 700 °C exhibited band gap value of 3.09 eV, 3.13 eV and 3.16 eV respectively. This increase in the band gap of ZnO with the increasing calcination temperature was attributed to the enhancement of particle size with the rise in calcination temperature. Table IV shows the variation in crystallite size, particle size and band gap energy with the change in calcination temperature.

R. Ashraf et al.[80] also reported sol-gel synthesized ZnO nanoparticles and investigated the effect of calcination temperature on its structural as well as optical properties. Zinc acetate dihydrate, DI water, IPA, triethyl acetate and sodium hydroxide were used for synthesis. The synthesized ZnO sample was calcined at various temperatures from 100 °C–500 °C. Figure 15 shows the XRD graph that confirmed the presence of pure phase hexagonal wurtzite ZnO structure. Further, Debye-Scherer formula was used to calculate the crystallite size of the prepared particles.

Figure 16 shows the plot of crystallite size obtained Vs calcination temperature. As the prepared ZnO sample was subjected to calcination, with the rise in temperature from 100 °C to 300 °C, the crystallite size was observed to decrease from 24 nm to 17 nm. However, when the temperature was further increased to 500 °C, the crystallite size was found to increase. The decline in crystallite size at a temperature less than 300 °C was implied to the restructuring process and the increase in crystallite size at a temperature more than 300 °C was implied to the strengthening of ZnO phase.

It was further observed that the calcination temperature robustly affects the transmission of sol-gel synthesized ZnO as can be seen in Fig. 17a. As the calcination temperature increased, the transmission of ZnO also increased. The utmost transmission of nearly 78% was obtained for the sample that was subjected to calcination at 300 °C. The band gap energy as shown in Fig. 17b was also found to increase from 3.39 eV to 3.41 eV with the rising calcination temperature.

A. Sangeetha et al.[81] investigated the significance of various calcination temperatures on structural, morphological and optical properties of ZnO. ZnO nanoparticles were synthesized via sol-gel system taking precursors zinc nitrate and sodium hydroxide and DI water as a solvent. Five samples of ZnO powder were obtained (as-synthesized ZnO and ZnO powder subjected to calcination in air at 200 °C, 500 °C, 700 °C, and 900 °C) for characterization. Nonappearance of
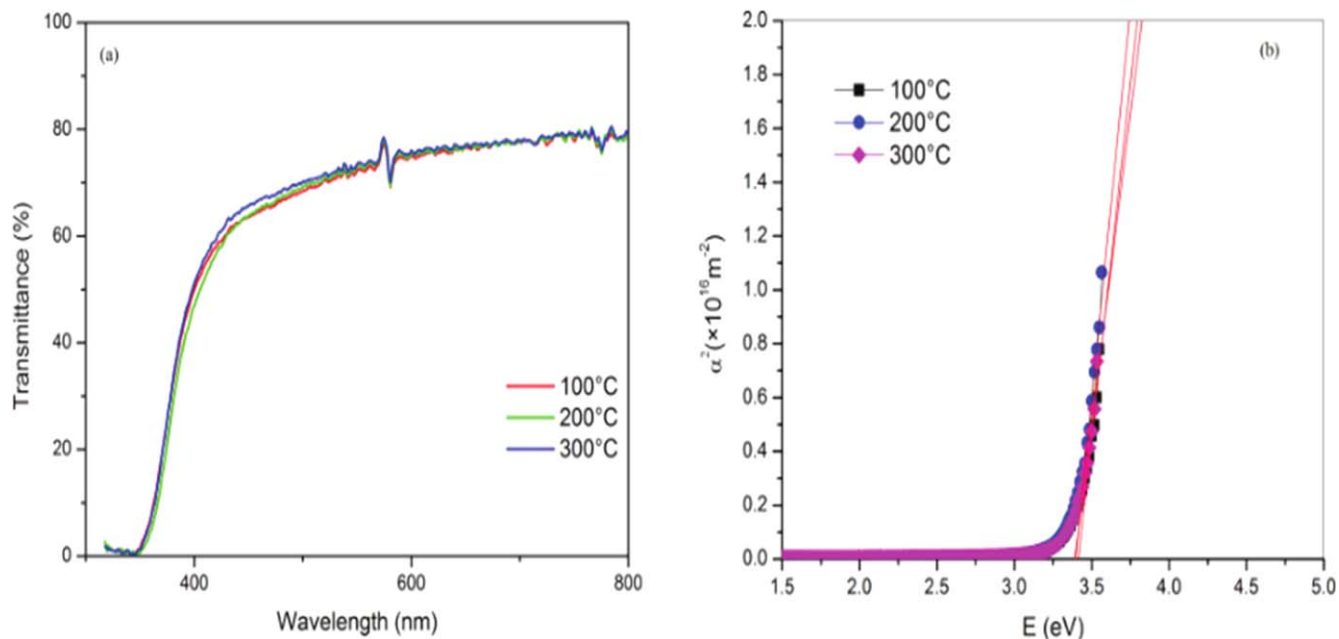
Figure 17. (a) Transmission plot, (b) Optical band gap energy of the synthesized samples at various calcination temperatures. Reproduced from Ref. 80 with permission, Copyright@2015, Elsevier.

considerable peaks subsequent to diffraction plane of ZnO was observed for as-prepared ZnO sample which indicated that as-prepared samples were amorphous in nature. However, significant crystalline peaks were observed for all the calcined samples indicating their polycrystalline hexagonal wurtzite structure. It was observed from the graph that up to 700 °C, the diffraction peak intensity increased which suggested the enhancement in crystallinity and strengthening of ZnO phase. At 700 °C, the highest crystalline peaks were obtained. Deterioration in the crystallinity of ZnO nanoparticles was observed at a further higher temperature of 900 °C as a consequence of the fast growth rate that led to the creation of defects.[82] It was further mentioned that calcination temperature affects the morphology of synthesized nanoparticles. At low temperature, ZnO nanoparticles exhibited plate-like morphology which progressively changed into inclusive nanorods at 700 °C with low aggregation and ample particle distribution. The band gap energy was found to be 3.3 eV at 200 °C, 3.4 eV at 500 °C and 3.48 eV at 700 °C. The band gap was observed to increase which was attributed to quantum confinement effect.[83]

Influence of capping agent.—Capping agents or surfactants are used for controllable synthesis of nanoparticles by adjusting the size and morphology of synthesized nanoparticles.[84–86] These capping agents or surfactants have structures consisting of lengthy hydrocarbon chains and their ends are hydrophobic. This structure is supposed to play a significant function in manipulating particle sizes.[87] There is a tendency of nanoparticles suspension to agglomerate which act as an obstacle in many applications served by them. In order to get rid of this hindrance, surface modification of ZnO and other nanoparticles is done by capping agents.[88–90] Sol-gel synthesis accompanied with capping agent acts as one of the simple and effective means for achieving a controllable synthesis. The accumulation of the capping molecule can affect the size confinement of ZnO, thereby influencing the physical properties of ZnO nanoparticles. Considerable variation in particle size is observed through the accumulation of capping agent. Conversely, there are other factors also that affect ZnO growth mechanism like pH, reaction temperature etc.[91,92]

P. Chandrasekaran et al.[93] in their work investigated the effect of capping agent on the size as well as the morphology of sol-gel synthesized ZnO nanoparticles. Zinc acetate dihydrate, sodium hydroxide and DI water were used for the preparation of different samples. In this study, three capping agents were used i.e. ethylene

diamine tetra acetic acid (EDTA), triethanolamine (TEA) and tetraethylammonium bromide (TEABr). XRD results confirmed the wurtzite crystal structure of ZnO nanoparticles. TEM images revealed that uncapped ZnO nanoparticles had no specific morphology. Moreover, the particles were observed to be well aggregated as shown in Figs. 18a, 18b. It was observed that EDTA capped ZnO nanoparticles were highly dispersed with size varying from 20 to 25 nm and exhibiting hexagonal morphology (Figs. 18c, 18d). EDTA has six reaction sites with four −OH groups that form coordination bonds with Zn^{2+} ions; thereby modifying the size as well as the morphology of ZnO nanoparticles. EDTA capped ZnO nanoparticles emerged with hexagonal morphology due to the six reaction sites of EDTA.[94] It was observed that TEA capped nanoparticles were monodispersed with size varying from 25 to 30 nm and exhibiting triangular like morphology (Figs. 18e, 18f). TEA has three reaction sites with −OH groups that were believed to network with Zn^{2+} ions in sol-gel medium, thereby modifying the morphology of ZnO nanoparticles. TEABr capped nanoparticles (Figs. 18g, 18h) were extremely distributed with size in the range of 20 nm to 25 nm. No particular morphology was observed in TEABr capped ZnO nanoparticles even though only some of them exhibited a somewhat distorted triangle like morphology. There are four alkyl groups with nitrogen in TEABr so the interaction of TEABr with Zn^{2+} ions in the sol-gel medium was weak in comparison to EDTA and TEA resulting in no specific morphology of TEABr capped ZnO. Thus, we can say that the morphology of sol-gel synthesized ZnO is influenced by capping agents due to the interaction between different reaction sites of organic molecules and Zn^{2+} ions of zinc acetate in the sol-gel medium. Further, it was also investigated how the concentration of capping agent affects the morphology of ZnO nanoparticles. For this, three samples of TEA capped ZnO were prepared where the addition of TEA was done with three different concentrations 0.2, 0.5 and 0.7 M. The morphology of ZnO nanoparticles does not exhibit any change with change in concentration of TEA (capping agent). Figure 19 describes the UV–vis spectra of ZnO and capped ZnO. It was observed that all the synthesized samples demonstrated outstanding UV absorption with a strong peak in the range 365–370 nm. Moreover, high transparency in the visible region can also be seen clearly in the figure. As compared to uncapped ZnO, TEA capped ZnO showed sharply increased absorption. Further, a slight increase in absorption was
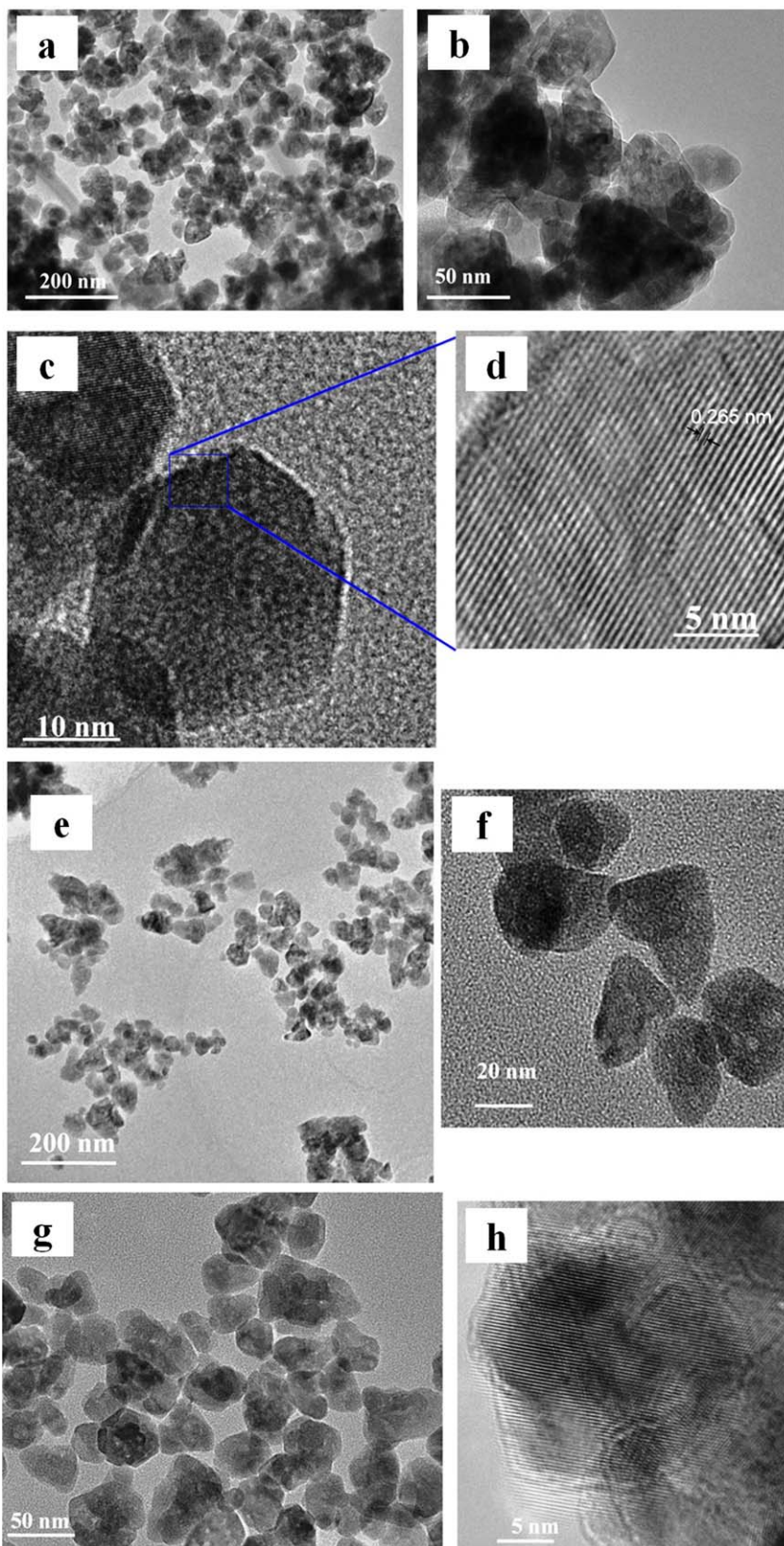
Figure 18. TEM images of (a), (b) uncapped ZnO, (c), (d) EDTA capped ZnO, (e), (f) TEA capped ZnO and (g), (h) TEABr capped ZnO. Reproduced from Ref. 93 with permission, Copyright@2012, Elsevier.

observed for TEABr capped ZnO in comparison to TEA capped ZnO. On the other hand, the highest absorption was demonstrated by EDTA capped ZnO in comparison to uncapped and other capped ZnO samples.

Suman et al.[95] synthesized various ZnO nanostructures by taking three capping agents. Zinc acetate dihydrate, sodium hydroxide and distilled water were taken as precursors while the different capping agents used were sodium dodecyl sulphate (SDS), trisodium citrate and cetyl trimethyl ammonium bromide (CTAB). Different samples were prepared for investigation viz. ZnO, trisodium citrate assisted ZnO (ZTrisodium), CTAB assisted ZnO (ZCTAB) and SDS assisted ZnO (ZSDS). From XRD data, it can be seen that the samples
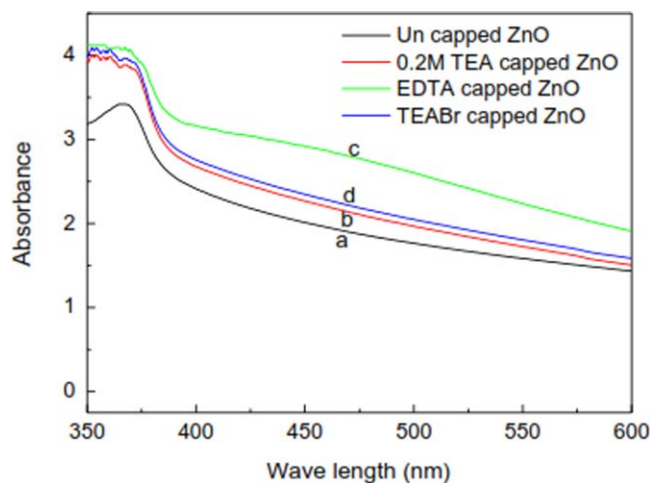
Figure 19. UV–vis spectra of uncapped and capped ZnO. Reproduced from Ref. 93 with permission, Copyright@2012, Elsevier.

demonstrated excellent crystallinity as shown in Fig. 20 and were single-phase hexagonal wurtzite structure. The estimated crystallite size was 23.10 nm for ZnO, 23 nm for ZCTAB, 18.20 nm for ZTrisodium and 16.14 nm for ZSDS. The investigation of morphology was done through FESEM. The Disc or plate-like morphology was observed for uncapped ZnO as shown in FESEM micrographs (Fig. 21a). For ZTrisodium, flower-like morphology of ZnO consisting of many hierarchal flowers like nanostructures assemblage was observed (Figs. 21b). For ZCTAB, numerous flower-shaped nanostructures were observed which resulted due to the assembly of a large number of ZnO nanoflakes that formed from a single axis (Fig. 21c). ZSDS (Fig. 21d) has shown spherical morphology and aggregation of particles. This study proves that the addition of surfactants influences the morphology of ZnO nanostructures.

While analyzing the absorption spectra of ZnO (Fig. 22), the absorption bands were observed at 374 nm, 365 nm, 371 nm and 367 nm respectively for uncapped ZnO, ZTrisodium, ZCTAB and ZSDS. It was observed that the absorption peaks of capped ZnO samples decreased in comparison to uncapped ZnO. Figs. 23a–23d shows the Sigmoidal fit for ZnO, ZTrisodium, ZSDS and ZCTAB. The energy band gap estimated from the graphs was found to be 3.30 eV, 3.34 eV, 3.32 eV and 3.31 eV respectively.

Effect on Photoluminescence Properties

In this section, the influence of different synthesis conditions on the photoluminescence (PL) properties of sol-gel synthesized ZnO nanoparticles is discussed. Rauwel et al.[96] studied the effect of hydrates in the zinc precursor ($Zn(acac)_2$, xH_2O) during the synthesis of ZnO nanoparticles by sol-gel method that was done in a glovebox. A mixture of 20 ml of benzyl amine and zinc acetylacetonate hydrate or zinc acetate was prepared and transferred to a stainless steel autoclave. The autoclave was then carefully sealed and taken out of the glovebox. Afterwards, it was subjected to heating at 200 °C for 2 d. The resultants were finally centrifuged, washed and then dried in air at 60 °C. Thus, two samples of ZnO nanoparticles were synthesized, one using zinc acetylacetonate hydrate (sample A) and other by zinc acetate (sample B). The PL spectra of bulk ZnO and the prepared samples of ZnO nanoparticles as shown in Fig. 24 were compared and studied. In the bulk ZnO spectra, suppressed band-edge luminescence was observed while in case of ZnO nanoparticles, broad visible emission was found to be noticeably enhanced. Both the PL spectra and the band edge of sample B are closer to bulk ZnO. This demonstrated a distinct direct optical transition with a characteristic excitonic absorption peak along with optical energy gap of 3.28 eV for sample B. On the contrary, a red-shift was observed in the absorption edge for sample A (3.2 eV) in comparison to bulk ZnO. Moreover, the absorption tail for sample A was stretched throughout the visible range.

S. Tachikawa et al.[97] explored the manipulation of polymer capping on the optical properties of sol-gel synthesized ZnO nanoparticles. Zinc acetate dihydrate, sodium hydroxide, ethanol and hexane were taken as precursors during synthesis while polyethylene glycol (PEG) and polyvinyl pyrrolidone (PVP) were added as polymer capping agents. While investigating how the polymer capping influences the optical properties of ZnO nanoparticles, the type of polymer and time of addition of polymer were mainly kept under consideration. When the polymer was added to
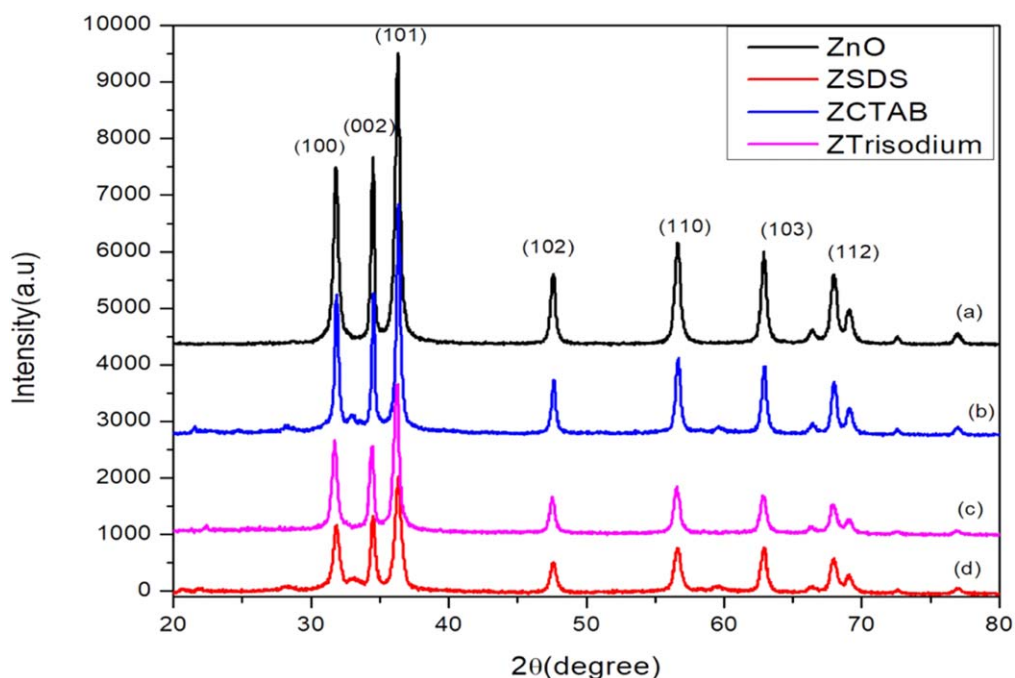

Figure 20. XRD of uncapped and capped ZnO. Reproduced from Ref. 95 under Creative Commons Attribution 3.0 license, Copyright@2020, IOP Science.
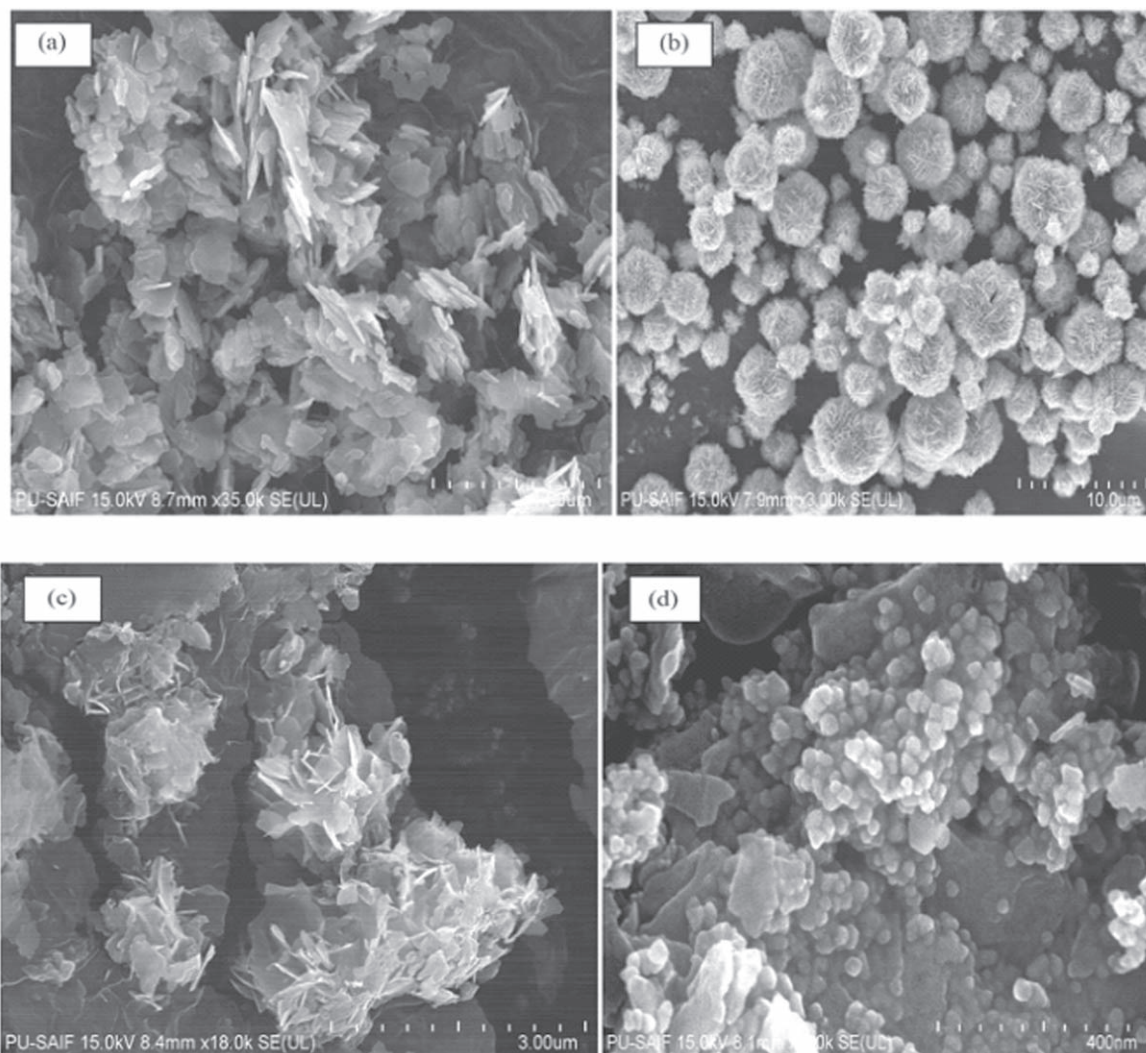
Figure 21. FESEM micrographs of (a) ZnO, (b) ZTrisodium, (c) ZCTAB and (d) ZSDS. Reproduced from Ref. 95 under Creative Commons Attribution 3.0 license, Copyright@2020, IOP Science.

the precursor ZnO solution before its synthesis, it was referred to as "before synthesis." On the contrary, "after synthesis" implied the addition of capping agent into the solution after the synthesis of ZnO. While analyzing the absorption spectrum for PEG, the results were compared by taking the case of "no addition of PEG" as the reference level. Figures 25a, 25b describes the schematic of ZnO nanoparticles capped by polymer molecules while Fig. 25c, 25d shows the PL spectra of the synthesized ZnO nanoparticles under an excitation wavelength of 300 nm. It was observed that by adding PEG in the solution at the time when ZnO nanoparticles were not formed, the total particle size increased and the fluorescence intensity also increased which indicates that capping has, in turn, resulted in surface passivation. On the contrary, the particle size and fluorescence were not changed by adding PEG in the solution subsequent to the formation of ZnO. Similar investigations were done with PVP. By adding PVP in the solution prior to the formation of ZnO nanoparticles, agglomeration of nanoparticles was observed. However, the particle size and fluorescence were observed to increase by adding PVP in the solution following the formation of ZnO. It was observed that capping the ZnO nanoparticles with PEG and PVP polymers enhanced the fluorescent efficiency of ZnO nanoparticles. So, we can conclude that the fluorescent intensity of ZnO nanoparticles can be increased by adding PEG before synthesis while adding PVP after synthesis. Further, as shown in Fig. 25e, there was a slight decrease in absorption edge as well as height for

PEG addition "before synthesis" while there was no change observed in absorption spectrum for PEG addition "after synthesis." Particle size as estimated from absorption edges were 3.7 nm (no addition of PEG), 3.8 nm (before synthesis) and 3.7 nm (after synthesis). Similarly, for PVP, there was a slight decrease in absorption edge as well as height for PVP addition "before synthesis" compared to "no addition of PVP." However, for PVP addition "after synthesis," it was observed that the absorption height decreased and absorption edge remains unchanged (Fig. 25f). The particle size as estimated from absorption edges were 3.8 nm (no addition of PVP), 3.6 nm (before synthesis), 3.8 nm (after synthesis).

Parra et al.[98] studied the effect of calcination temperature on the PL properties of sol-gel synthesized ZnO nanoparticles that were prepared using precursors zinc acetate dihydrate and sodium hydroxide. In this study, the resultant precipitates were calcined at 200 °C, 400 °C and 500 °C. The PL spectra of the synthesized samples as shown in Fig. 26, demonstrated three emission bands. At 3.2 eV, a strong UV emission peak was observed corresponding to exciton recombination associated with near band edge emission of ZnO. At 2.97 eV, an extremely weak violet emission peak was seen attributed to electron and hole recombination lying at zinc interstitial and in the valance band respectively. Further, at 2.60 eV, the observed week blue emission is related to transition of the electron from conduction band to interstitial oxygen defects in the ZnO. The quality of the synthesized ZnO nanoparticles can be evaluated by the intensity
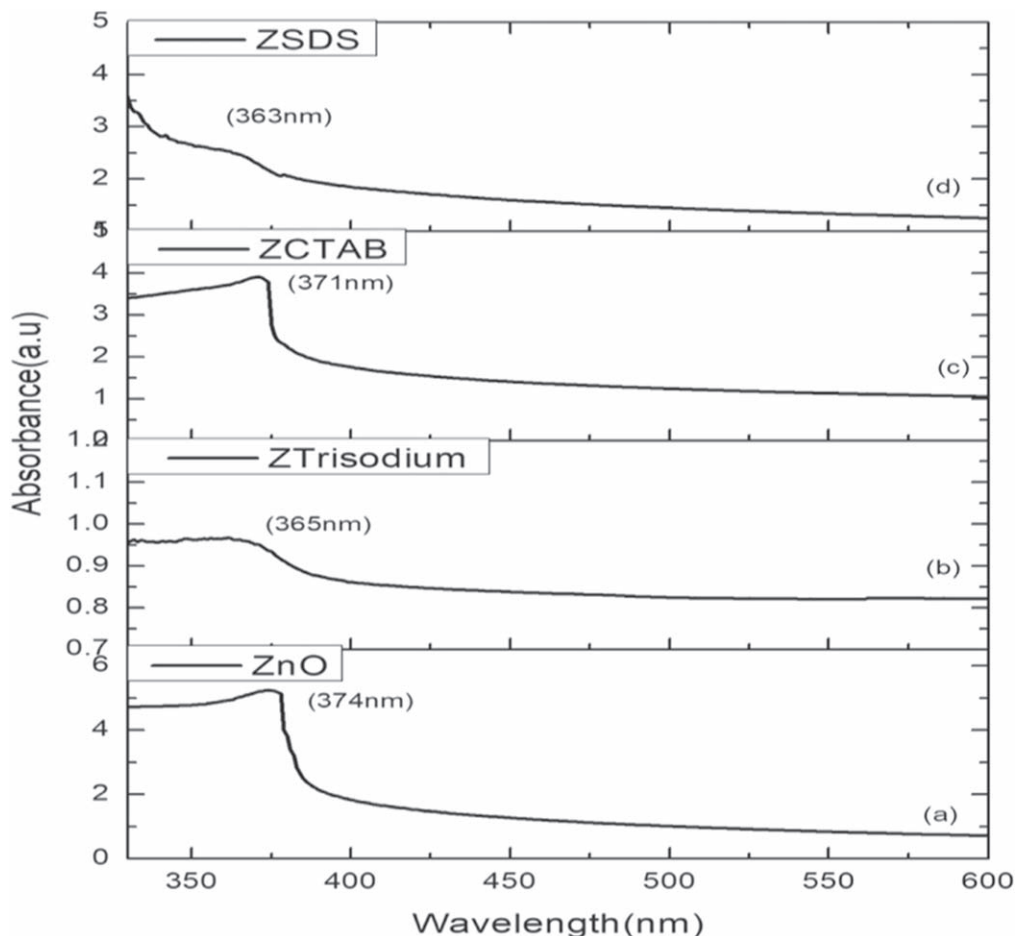
Figure 22. Absorption spectra of uncapped and capped ZnO. Reproduced from Ref. 95 under Creative Commons Attribution 3.0 license, Copyright@2020, IOP Science.

ratio between the near band edge UV emission and the visible emission. From the PL spectra, it can be clearly seen that the nanoparticles calcined at higher temperatures demonstrated sharp and narrow UV emission peaks with high intensities in comparison to visible emission peaks. Consequently, there is a red shift in the optical bandgap as the calcination temperature increases from 200 °C to 500 °C. Thus, it can be concluded that the crystallinity increased and defect density decreased with the increasing calcination temperatures due to higher ultraviolet emission peaks observed at higher calcination temperatures.

Verma et al.[99] studied the influence of capping and annealing on the optical properties of ZnO nanoparticles. Two samples were prepared i.e. uncapped ZnO nanoparticles and polyvinyl alcohol (PVA) capped ZnO nanoparticles. The samples were further annealed at temperatures of 200 °C, 400 °C, 500 °C and 600 °C for 2 h in air. The PL spectra were taken at excitation wavelengths of 225 and 330 nm. Figures 27a, 27b shows the PL emission spectra of the prepared samples taken at 225 nm excitation and it clearly demonstrates a sharp excitonic peak at ∼380 nm in the UV region which is due to band edge emission of ZnO. However, as the calcination temperature increased from 200 °C to 600 °C, a slight red shift was seen which is attributed to the increased particle size and decreased bandgap energy with an increase in annealing temperature. For uncapped ZnO, the peak shifted from 387 to 392 nm while for PVA capped ZnO, the peak shifted from 389 to 394 nm with the rise in temperature. Nevertheless, the shift can also be due to the stress developed in the samples as a result of annealing. The PL spectra taken at 330 nm excitation is shown in Figs. 27c, 27d which demonstrates defect related visible PL emission bands besides the band edge UV emission. For uncapped ZnO, the UV peak shifted

from 372 to 385 nm while for PVA capped ZnO, the peak shifted from 371 to 383 nm with the rise in temperature. Figure 27d revealed that S2#600 has strongest UV PL emission peak that may be a consequence of increased crystallinity of the sample at higher annealing temperature. The peak at 421 nm is a resultant of the transition from zinc interstitial to the valence band while the blue emissions at 445, 460, and 487 nm are the resultants of the transitions from extended zinc interstitial states to the valence band. Further, the broad green band at 530 nm is a resultant of the transition between conduction band and the energy levels formed with oxygen substitution at zinc vacancies. Figure 27e shows the energy level diagram demonstrating different transitions responsible for PL emissions.

Challenges in The Sol-Gel Method of Synthesis

There are a variety of methods available for synthesizing ZnO nanoparticles which are divided into physical, chemical and biological processes. The chemical methods are further divided into liquid phase and gas-phase synthesis. Various methods that come under liquid phase synthesis are sol-gel process, colloidal methods, precipitation, water-oil microemulsions method, coprecipitation method, solvothermal method, hydrothermal method. Gas-phase techniques include pyrolysis and inert gas condensation method.[100] Figure 28 shows the most important synthetic techniques that have been employed for ZnO nanoparticles synthesis. Since the chemical method of synthesis depends on the consumption of chemicals, the large scale production of nanoparticles via chemical methods has led to an increase in environmental contamination due to the release of undesired chemicals in the ecosystem during the chemical synthesis process of nanoparticles.[101]
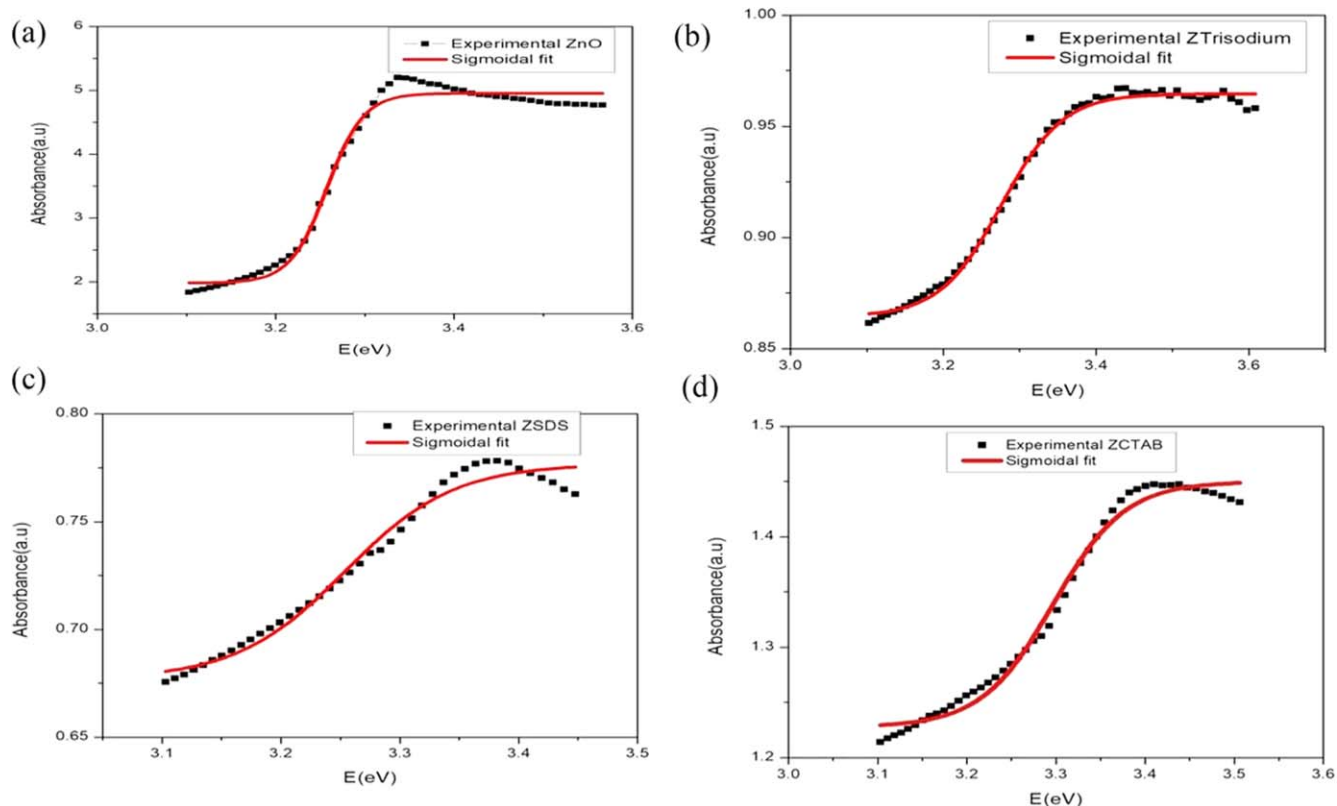
Figure 23. Graphs showing Sigmoidal fit for (a) ZnO, (b) ZTrisodium, (c) ZSDS and (d) ZCTAB. Reproduced from Ref. 95 under Creative Commons Attribution 3.0 license, Copyright@2020, IOP Science.
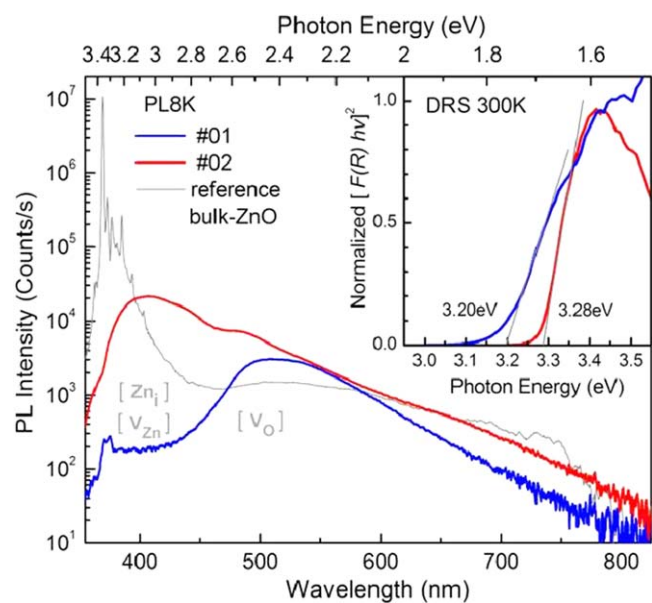

Figure 24. PL spectra of reference bulk ZnO, sample A (curve #01) and sample B (curve #02) ZnO nanoparticles while inset shows the corresponding obtained band gap energy. Reproduced from Ref. 96 with permission, Copyright@2011, American Chemical Society.

In order to overcome the harmful impact caused by the release of chemicals during the synthesis of nanomaterials via chemical methods of synthesis, sustainable Green-synthesis approach for nanomaterial synthesis is developing. Though Green-synthesis route helps in reducing environmental hazards, it also has its own

limitations too. The significant point which is worth to consider is the instability observed in the nanoparticles that are synthesized by Green-synthesis approach. Unusual superfluous chemical moieties may form as a result of variation in the confirmation or arrangement of the biosynthesized nanoparticles caused by their physical instability. This instability may arise through a variety of diverse conditions for instance, light, pressure, pH, temperature, medium, and so on.[100] Another important concern is the intrinsic toxicity of ZnO nanoparticles arising by this approach that is associated with dissolution and reactive oxygen species (ROS) generation. Between these two, dissolution is the foremost phenomenon leading to the biological as well as the chemical instability of ZnO. There are two driving forces for the dissolution of ZnO nanoparticles, one is the concentration gradient between the bulk solution phase and particle surface, and other is the metal solubility. This effect may result in the formation of highly noxious Zn^{2+} and $Zn(OH)^{+}$.[102] However, there are various factors by which dissolution phenomenon can be controlled. These may include doping, coating of nanoparticles, surface area effect, and other approaches like size-dependent variation of the surface curvature, and roughness of the particles. Furthermore, due to the redox reaction that occurs on the nanoparticles surface simultaneously, the crystalline nature of the nanoparticles may also vary. During these reactions, the transfer of electrons generates ROS and oxidative stress leading to toxicological injury.[103] As a consequence, the dilemma of dissolution of ions and ROS generation may act as an impending hazard to the contiguous surroundings. Chemically synthesized nanoparticles are significantly stable but the green synthesized nanoparticles, on the other hand are quite less stable.

Biosynthesis of ZnO nanoparticles using sol-gel method..—With the aim of reducing the load of environmental pollution, green routes of ZnO nanoparticles preparation is gaining popularity.
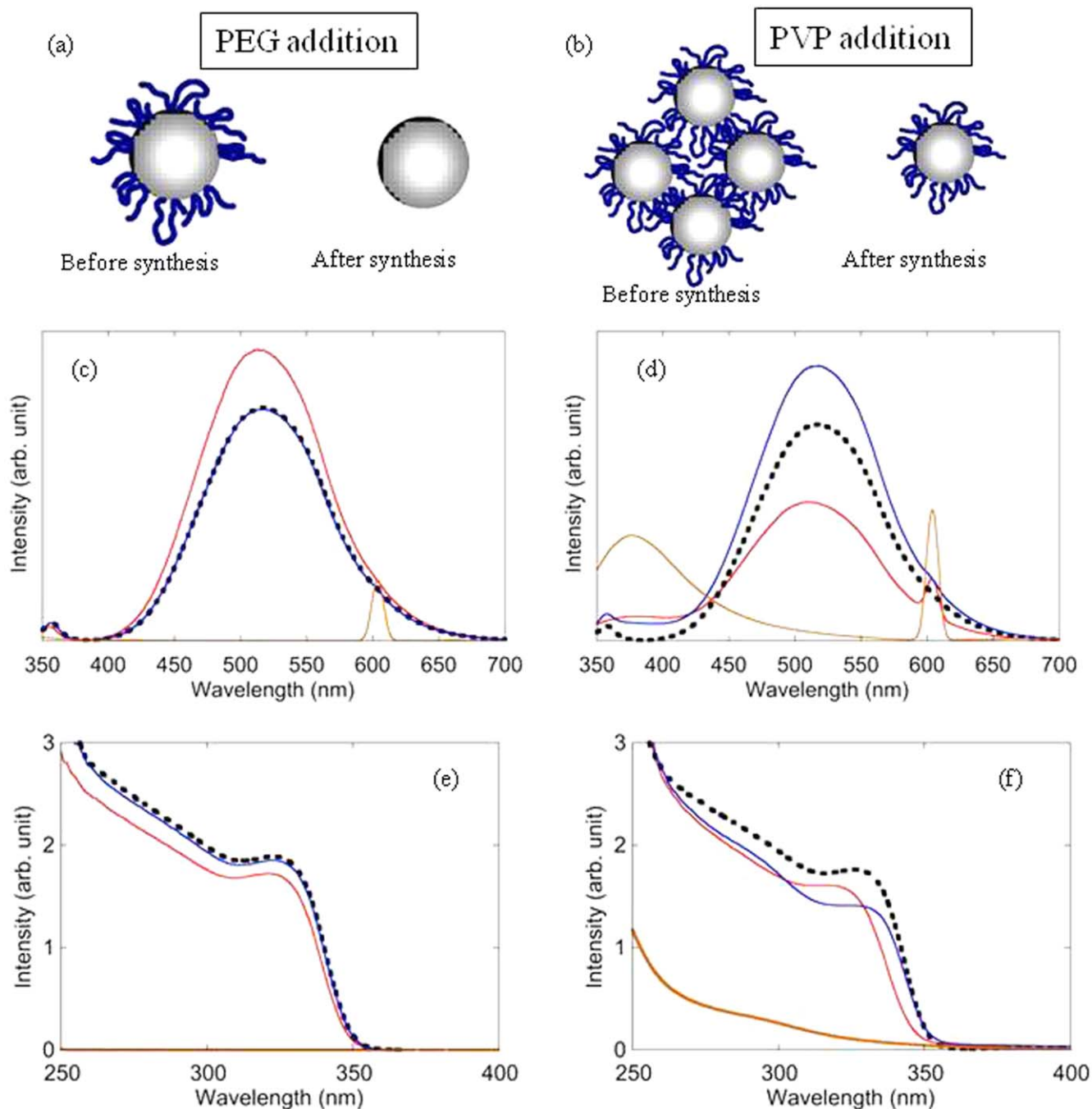
Figure 25. (a), (b) Schematic diagram showing the capping of ZnO nanoparticles by polymer molecules before and after synthesis, (c), (d) Photoluminescence spectra of ZnO solution under an excitation wavelength of 300 nm, (e), (f) UV spectra of ZnO solution. Black dotted line: "No addition," Red line: "before synthesis," Blue line: "after synthesis," Brown line: spectra of the polymer solution. Reproduced from Ref. 97 under Creative Commons Attribution 3.0 license, Copyright@2011, MDPI.

Owing to the less use of chemicals during the synthesis process, green synthesis reduces the number of pollutants. Moreover, this is energy-efficient and cost-effective means of synthesis of nanoparticles.[100] Plants extracts can be used for the synthesis of metal nanoparticles in environmental friendly approach, thereby reducing the risks of using hazardous chemicals in the synthesis process. This methodology of synthesis is cost-effective and simple.[104,105] Microbes are also used in the synthesis of nanoparticles. It is one of the sustainable and environment friendly methods of synthesis. Interaction involving microbes and metals has been explored for a number of biological applications like biocorrosion, bioleaching, bioremediation and biomineralization.[106]

N.A. Samat and R.M. Nor[107] reported the biosynthetic sol-gel route of ZnO nanoparticles synthesis using Citrus aurantifolia extracts (by using plant extract), in an ecological and lucrative manner. In this process, Citrus aurantifolia extract (pulp blended in DI water) with Zinc acetate at different concentration was used to prepare ZnO nanoparticles. XRD data revealed the formation of hexagonal wurtzite ZnO structure (Fig. 29). The size of the synthesized ZnO nanoparticles was obtained to be 50–200 nm. Figure 30 shows the SEM of prepared ZnO nanoparticles. This strategy of using Citrus aurantifolia extract was demonstrated and proposed as a good substitute for synthesizing ZnO nanoparticles using biomaterials.
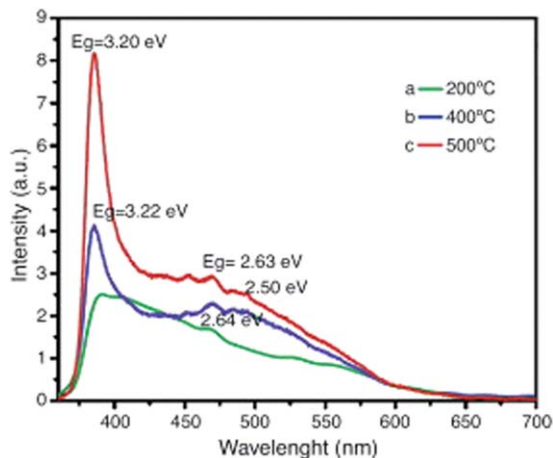
Figure 26. PL spectra of the synthesized samples at various calcination temperatures. Reproduced from Ref. 98 under Creative Commons Attribution 4.0 License, Copyright@2014, Brazilian Metallurgical, Materials and Mining Association.

Sol-gel Method Incorporated With Other Technologies for the Synthesis of Nanoparticles

The performance of a material in a particular application is greatly determined by the morphology, crystal structure as well as size distribution.[108] ZnO nanoparticles have been studied comprehensively on account of their size-dependent optical and electronic properties.[109] Various techniques have been investigated for synthesizing ZnO nanoparticles, among them sol-gel method is popular owing to its inexpensive, effortlessness, reproducibility and reliability of stoichiometry control. This technique offers control on morphology and grain size of synthesized nanoparticles through suitably and carefully regulating the experimental conditions during synthesis process.[110]

In order to achieve controlled morphology, unique microstructure and improved properties, the sol-gel process incorporated with other techniques are used. These modified and improved sol-gel routes of synthesis could be achieved by incorporating spray-drying, in situ doping or surface modification. These recent developments in synthesis process are extensively employed to synthesize pure nanoparticles or nanopowders; in consequence of their potential to manage the particle size, morphology, uniformity, size distribution,
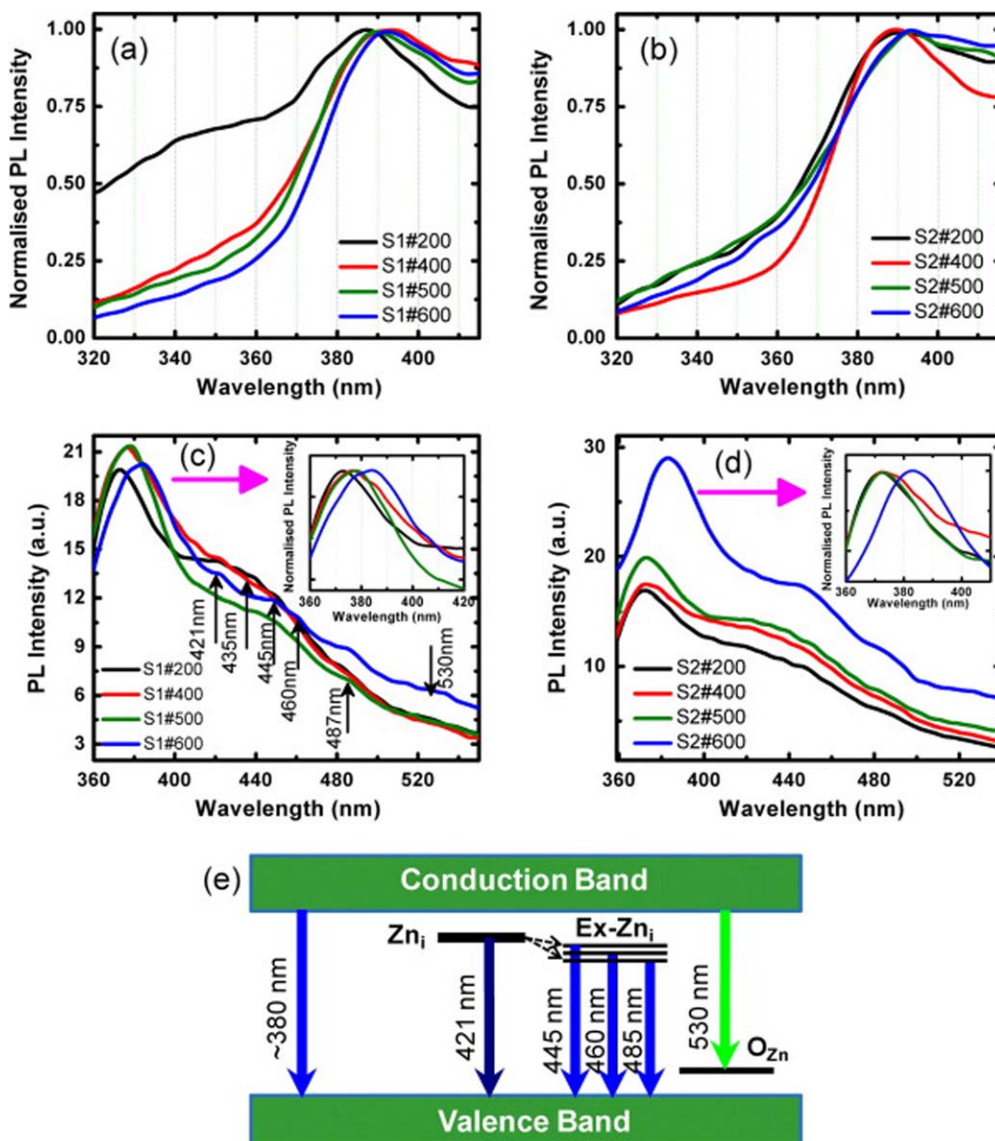

Figure 27. (a), (b) Normalized PL emission spectra of uncapped ZnO and PVA capped ZnO taken at 225 nm excitation, (c), (d) PL emission spectra of uncapped ZnO and PVA capped ZnO taken at 330 nm excitation and (e) Energy level diagram demonstrating different transitions responsible for PL emissions. Reproduced from Ref. 99 with permission, Copyright@2014, Elsevier B.V.

Figure 28. Most important synthetic techniques employed for ZnO nanoparticles synthesis. Reproduced from Ref. 100 under Creative Commons Attribution 3.0 license, Copyright@2017, Hindawi.
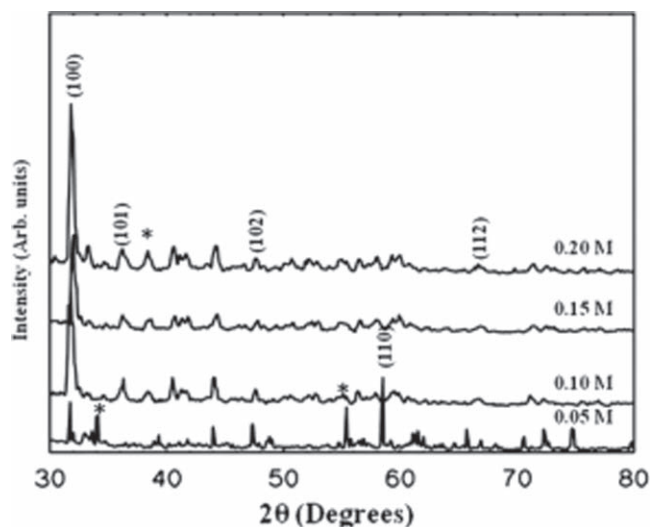

Figure 29. XRD graphs of ZnO nanoparticles synthesized by taking different concentrations of zinc acetate. Here, peaks labelled as star implies peaks of $Zn(OH)_2$. Reproduced from Ref. 107 with permission, Copyright@2013, Elsevier.

and agglomeration by systematically examining the process parameters and resourcefully utilizing the dispersion mechanism. The sol-gel method incorporated with spray-drying, in situ doping and surface modification is used to produce monodispersed nanoparticles for enhancing the microstructure, sintering characterization, mechanical and dielectric properties of electroceramic and structural ceramics caused by remarkable nanosize effect.[111–117]

Conclusions

There are a lot of developments undergoing to achieve controlled morphology, tailoring of the band gap, exploration of unique and superior properties of nanomaterials so that they can be used in a better way in special application areas. ZnO nanostructures offer an extensive variety of applications as a result of their peculiar properties. Though many techniques are accessible for synthesizing ZnO nanoparticles; in this review, we have tried to explore the synthesis of ZnO nanoparticles via sol-gel method. There are several processing parameters concerned during the synthesis of nanomaterials using the sol-gel process which affect the properties of the synthesized material. In that way, an understanding of the parameters involved during the synthesis process of nanomaterials plays a vital function. In this review article, the role of processing parameters during the synthesis of ZnO nanoparticles via the sol-gel method is emphasized. The control of processing parameters like pH of sol, capping agent, calcination and annealing temperature on ZnO nanoparticles are studied here. As reviewed from the available literature, it is observed that the pH of the sol affects the particle size as well as optical band gap energy. Selective control of the pH of the solution can alter the size and optical properties of ZnO nanoparticles. Calcination and annealing temperature also plays an essential part in tailoring the size, shape and optical properties of ZnO
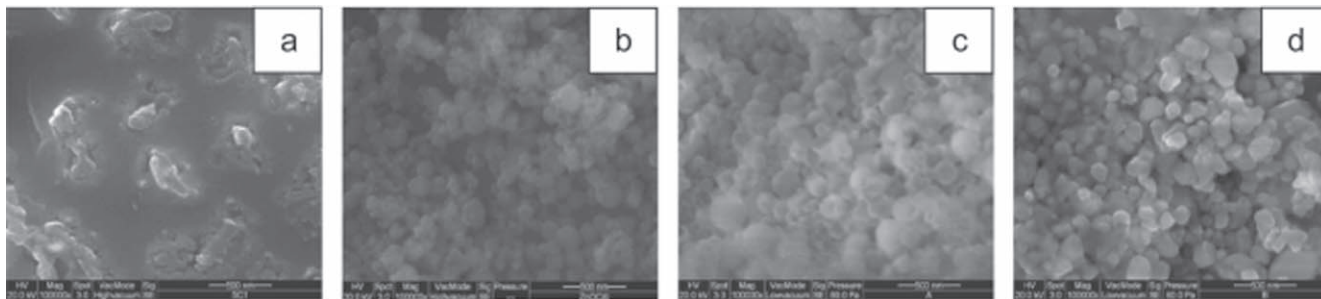
Figure 30. SEM images of ZnO prepared by taking different concentrations of zinc acetate (a) 0.05 M, (b) 0.10 M, (c) 0.15 M and (d) 0.20 M. Reproduced from Ref. 107 with permission, Copyright@2013, Elsevier.

nanoparticles synthesized via sol-gel process. Introduction of additive like capping agents/surfactants also affects the morphology and optical properties of synthesized ZnO nanoparticles. By carefully adjusting these parameters under systematic monitoring, we can yield better and desired results that could be helpful in various application areas like biomedical and optoelectronics etc.

ORCID

Sandeep Arya https://orcid.org/0000-0001-5059-0609
Ajit Khosla https://orcid.org/0000-0002-2803-8532
Vinay Gupta https://orcid.org/0000-0003-3223-7267
Sai Kiran Oruganti https://orcid.org/0000-0003-4601-2907

References

1. D. Segets, J. Gradl, R. K. Taylor, V. Vassilev, and W. Peukert, "Analysis of optical absorbance spectra for the determination of ZnO nanoparticle size distribution, solubility, and surface energy." *ACS Nano*, **3**, 1703 (2009).
2. L. Xiangdong, S. Hesheng, and S. Yusheng, "The development of ZnO series ceramic semiconductor gas sensors." *J. Trans. Technol.*, **3**, 1 (1991).
3. P. B. Lihitkar, S. Violet, M. Shirolkar, J. Singh, O. N. Srivastava, R. H. Naik, and S. K. Kulkarni, "Confinement of zinc oxide nanoparticles in ordered mesoporous silica MCM-41." *Mater. Chem. Phys.*, **133**, 850 (2012).
4. H. Kumar and R. Rani, "Structural and optical characterization of ZnO nanoparticles synthesized by microemulsion route." *International Letters of Chemistry, Physics and Astronomy*, **14**, 26 (2013).
5. E. Rauwel, A. Galeckas, M. R. Soares, and P. Rauwel, "Influence of the interface on the photoluminescence properties in ZnO carbon-based nanohybrids." *The Journal of Physical Chemistry C*, **121**, 14879 (2017).
6. T. Aoki, Y. Hatanaka, and D. C. Look, "ZnO diode fabricated by excimer-laser doping." *Appl. Phys. Lett.*, **76**, 3257 (2000).
7. D. Li, J. She, S. Xu, and S. Deng, "Zinc oxide nanowire lateral field emission devices and its application as display pixel structures." *IEEE Trans. Electron Devices*, **60**, 2924 (2013).
8. X. W. Sun, J. Z. Huang, J. X. Wang, and Z. Xu, "A ZnO nanorod inorganic/organic heterostructure light-emitting diode emitting at 342 nm." *Nano Lett.*, **8**, 1219 (2008).
9. S. Xu and Z. L. Wang, *Nano Res.*, **4**, 1013 (2011).
10. Z. L. Wang, "Splendid one-dimensional nanostructures of zinc oxide: a new nanomaterial family for nanotechnology." *Acs Nano*, **2**, 1987 (2008).
11. M. Chaari and A. Matoussi, "Electrical conduction and dielectric studies of ZnO pellets." *Physica B*, **407**, 3441 (2012).
12. Ü. Özgür, Y. I. Alivov, C. Liu, A. Teke, M. A. Reshchikov, S. Doğan, and A. H. Morkoç, "A comprehensive review of ZnO materials and devices." *J. Appl. Phys.*, **98**, 041301 (2005).
13. S. Bhattacharyya and A. Gedanken, "A template-free, sonochemical route to porous ZnO nano-disks." *Microporous Mesoporous Mater.*, **110**, 553 (2008).
14. B. Ludi and M. Niederberger, "Zinc oxide nanoparticles: chemical mechanisms and classical and non-classical crystallization." *Dalton Trans.*, **42**, 12554 (2013).
15. J. W. Rasmussen, E. Martinez, P. Louka, and D. G. Wingett, "Zinc oxide nanoparticles for selective destruction of tumor cells and potential for drug delivery applications." *Expert Opinion on Drug Delivery*, **7**, 1063 (2010).
16. H. M. Xiong, "ZnO nanoparticles applied to bioimaging and drug delivery." *Adv. Mater.*, **25**, 5329 (2013).
17. M. Al-Fori, S. Dobretsov, M. T. Z. Myint, and J. Dutta, "Antifouling properties of zinc oxide nanorod coatings." *Biofouling*, **30**, 871 (2014).
18. M. D. Newman, M. Stotland, and J. I. Ellis, "The safety of nanosized particles in titanium dioxide–and zinc oxide–based sunscreens." *Journal of the American Academy of Dermatology*, **61**, 685 (2009).
19. B. Liu and H. C. Zeng, "Hydrothermal synthesis of ZnO nanorods in the diameter regime of 50 nm." *JACS*, **125**, 4430 (2003).
20. C. X. Xu, A. Wei, X. W. Sun, and Z. L. Dong, "Aligned ZnO nanorods synthesized by a simple hydrothermal reaction." *J. Phys. D*, **39**, 1690 (2006).
21. S. Baruah and J. Dutta, "Effect of seeded substrates on hydrothermally grown ZnO nanorods." *J. Sol-Gel Sci. Technol.*, **50**, 456 (2009).
22. X. Y. Kong, Y. Ding, R. Yang, and Z. L. Wang, "Single-crystal nanorings formed by epitaxial self-coiling of polar nanobelts." *Science*, **303**, 1348 (2004).
23. L. E. Greene, M. Law, D. H. Tan, M. Montano, J. Goldberger, G. Somorjai, and P. Yang, "General route to vertical ZnO nanowire arrays using textured ZnO seeds." *Nano Lett.*, **5**, 1231 (2005).
24. L. E. Greene, B. D. Yuhas, M. Law, D. Zitoun, and P. Yang, "Solution-grown zinc oxide nanowires." *Inorg. Chem.*, **45**, 7535 (2006).
25. Z. W. Pan, Z. R. Dai, and Z. L. Wang, "Nanobelts of semiconducting oxides." *Science*, **291**, 1947 (2001).
26. P. X. Gao and Z. L. Wang, "Mesoporous polyhedral cages and shells formed by textured self-assembly of ZnO nanocrystals." *JACS*, **125**, 11299 (2003).
27. C. S. Lao, P. X. Gao, R. S. Yang, Y. Zhang, Y. Dai, and Z. L. Wang, "Formation of double-side teethed nanocombs of ZnO and self-catalysis of Zn-terminated polar surface." *Chem. Phys. Lett.*, **417**, 358 (2006).
28. S. Peulon and D. Lincot, "Cathodic electrodeposition from aqueous solution of dense or open-structured zinc oxide films." *Adv. Mater.*, **8**, 166 (1996).
29. J. J. Wu and S. C. Liu, "Catalyst-free growth and characterization of ZnO nanorods." *J. Phys. Chem. B*, **106**, 9546 (2002).
30. D. Sun, M. Wong, L. Sun, Y. Li, N. Miyatake, and H. J. Sue, "Purification and stabilization of colloidal ZnO nanoparticles in methanol." *J. Sol-Gel Sci. Technol.*, **43**, 237 (2007).
31. Y. Zhang, R. E. Russo, and S. S. Mao, "Quantum efficiency of ZnO nanowire nanolasers." *Appl. Phys. Lett.*, **87**, 043106 (2005).
32. H. Zhang, D. Yang, Y. Ji, X. Ma, J. Xu, and D. Que, "Low temperature synthesis of flowerlike ZnO nanostructures by cetyltrimethylammonium bromide-assisted hydrothermal process." *J. Phys. Chem. B*, **108**, 3955 (2004).
33. Z. B. Shao, C. Y. Wang, S. D. Geng, X. D. Sun, and S. J. Geng, "Fabrication of nanometer-sized zinc oxide at low decomposing temperature." *J. Mater. Process. Technol.*, **178**, 247 (2006).
34. V. V. Shinde, D. S. Dalavi, S. S. Mali, C. K. Hong, J. H. Kim, and P. S. Patil, "Surfactant free microwave assisted synthesis of ZnO microspheres: Study of their antibacterial activity." *Appl. Surf. Sci.*, **307**, 495 (2014).
35. B. Ebin, E. Arıg, B. Özkal, and S. Gürmen, "Production and characterization of ZnO nanoparticles and porous particles by ultrasonic spray pyrolysis using a zinc nitrate precursor." *Int. J. Miner. Metall. Mater.*, **19**, 651 (2012).
36. K. T. R. Reddy, V. Supriya, Y. Murata, and M. Sugiyama, "Effect of Co-doping on the properties of Zn1− xCoxO films deposited by spray pyrolysis." *Surf. Coat. Technol.*, **231**, 149 (2013).
37. R. He, B. Tang, C. Ton-That, M. Phillips, and T. Tsuzuki, "Physical structure and optical properties of Co-doped ZnO nanoparticles prepared by co-precipitation." *J. Nanopart. Res.*, **15**, 2030 (2013).
38. S. G. Kang, Y. Kim, S. E. Kim, and S. Kim, "The effects of heat treatment on room temperature ferromagnetism in a digitally Co doped ZnO thin film." *Electron. Mater. Lett.*, **9**, 7 (2013).
39. N. M. Shamhari, B. S. Wee, S. F. Chin, and K. Y. Kok, "Synthesis and characterization of zinc oxide nanoparticles with small particle size distribution." *Acta Chimica Slovenica*, **65**, 578 (2018).
40. M. F. Hossain, Z. H. Zhang, and T. Takahashi, "Novel micro-ring structured ZnO photoelectrode for dye-sensitized solar cell." *Nano-Micro Letters*, **2**, 53 (2010).
41. J. Aizpurua, P. Hanarp, D. S. Sutherland, M. Käll, G. W. Bryant, and F. G. De Abajo, "Optical properties of gold nanorings." *Phys. Rev. Lett.*, **90**, 057401 (2003).
42. M. S. Tokumoto, S. H. Pulcinelli, C. V. Santilli, and V. Briois, "Catalysis and temperature dependence on the formation of ZnO nanoparticles and of zinc acetate derivatives prepared by the sol− gel route." *J. Phys. Chem. B*, **107**, 568 (2003).
43. M. Vafaee and M. S. Ghamsari, "Preparation and characterization of ZnO nanoparticles by a novel sol–gel route." *Mater. Lett.*, **61**, 3265 (2007).
44. A. Kumar, N. Yadav, M. Bhatt, N. K. Mishra, P. Chaudhary, and R. Singh, "Sol-gel derived nanomaterials and it's applications: a review." *Research Journal of Chemical Sciences*, **5**, 98 (2015).
45. C. A. Milea, C. Bogatu, and A. Duta, "The influence of parameters in silica sol-gel process." *Bulletin of the Transilvania University of Brasov. Series I-Engineering Sciences*, **4**, 59 (2011).
46. N. Singh, Dhruvanshi, D. Kaur, R. M. Mehra, and A. Kapoor, "Effect of ageing in structural properties of ZnO nanoparticles with pH variation for application in solar cells." *The Open Renewable Energy Journal*, **5** (2012).

47. A. Collins, *Nanotechnology Cookbook: Practical, Reliable and Jargon-Free Experimental Procedures.* (Elsevier, Amsterdam) (2012).

48. G. V. Aguilar, "Introductory chapter: a brief semblance of the sol-gel method in research." *In Sol-Gel Method-Design and Synthesis of New Materials with Interesting Physical, Chemical and Biological Properties.* (IntechOpen)(United Kingdom) (2018).

49. S. Rani, P. Suri, P. K. Shishodia, and R. M. Mehra, "Synthesis of nanocrystalline ZnO powder via sol-gel route for dye-sensitized solar cells." *Sol. Energy Mater. Sol. Cells*, **92**, 1639 (2008).

50. S. Arya, M. Riyas, A. Sharma, B. Singh, P. Bandhoria, S. Khan, and V. Bharti, "Electrochemical detection of ammonia solution using tin oxide nanoparticles synthesized via sol-gel route." *Appl. Phys. A*, **124**, 538 (2018).

51. A.,. S. Prerna, A. Sharma, B. Singh, A. Tomar, S. Singh, and R. Sharma, "Morphological and optical characterization of sol-gel synthesized Ni-doped ZnO nanoparticles." *Integr. Ferroelectr.*, **205**, 1 (2020).

52. P. Mahajan, A. Singh, and S. Arya, "Improved performance of solution processed organic solar cells with an additive layer of sol-gel synthesized ZnO/CuO core/shell nanoparticles." *J. Alloys Compd.*, **814**, 152292 (2020).

53. P. Mahajan, A. Singh, R. Datt, V. Gupta, and S. Arya, "Realization of inverted organic solar cells by using sol-gel synthesized ZnO/Y₂O₃ Core/shell nanoparticles as electron transport layer." *IEEE J. Photovolt.*, **10**, 1744 (2020).

54. S. Esposito, "'Traditional' sol-gel chemistry as a powerful tool for the preparation of supported metal and metal oxide catalysts." *Materials*, **12**, 668 (2019).

55. J. Livage and D. Ganguli, "Sol-gel electrochromic coatings and devices: a review." *Sol. Energy Mater. Sol. Cells*, **68**, 365 (2001).

56. A. Sirelkhatim, S. Mahmud, A. Seeni, N. H. M. Kaus, L. C. Ann, S. K. M. Bakhori, and D. Mohamad, "Review on zinc oxide nanoparticles: antibacterial activity and toxicity mechanism." *Nano-Micro Letters*, **7**, 219 (2015).

57. D. P. Norton et al., "Charge carrier and spin doping in ZnO thin films." *Thin Solid Films*, **496**, 160 (2006).

58. Y. B. Hahn, "Zinc oxide nanostructures and their applications." *Korean J. Chem. Eng.*, **28**, 1797 (2011).

59. W. J. Li, E. W. Shi, W. Z. Zhong, and Z. W. Yin, "Growth mechanism and growth habit of oxide crystals." *J. Cryst. Growth*, **203**, 186 (1999).

60. T. Sekiguchi, K. Haga, and K. Inaba, "ZnO films grown under the oxygen-rich condition." *J. Cryst. Growth*, **214**, 68 (2000).

61. E. Gharoy Ahangar, M. H. Abbaspour-Fard, N. Shahtahmassebi, M. Khojastehpour, and P. Maddahi, "Preparation and characterization of PVA/ZnO nanocomposite." *J. Food Process. Preserv.*, **39**, 1442 (2015).

62. B. Kumar and S. W. Kim, "Energy harvesting based on semiconducting piezoelectric ZnO nanostructures." *Nano Energy*, **1**, 342 (2012).

63. M. Ristić, S. Musić, M. Ivanda, and S. Popović, "Sol-gel synthesis and characterization of nanocrystalline ZnO powders." *J. Alloys Compd.*, **397**, L1 (2005).

64. S. A. Akhoon, S. Rubab, and M. A. Shah, "A benign hydrothermal synthesis of nanopencils-like zinc oxide nanoflowers." *International Nano Letters*, **5**, 9 (2015).

65. H. Köse, Ş. Karaal, A. O. Aydın, and H. Akbulut, "A facile synthesis of zinc oxide/multiwalled carbon nanotube nanocomposite lithium ion battery anodes by sol-gel method." *J. Power Sources*, **295**, 235 (2015).

66. R. Wahab, S. G. Ansari, Y. S. Kim, M. Song, and H. S. Shin, "The role of pH variation on the growth of zinc oxide nanostructures." *Appl. Surf. Sci.*, **255**, 4891 (2009).

67. H. Zhang, D. Yang, X. Ma, Y. Ji, J. Xu, and D. Que, "Synthesis of flower-like ZnO nanostructures by an organic-free hydrothermal process." *Nanotechnology*, **15**, 622 (2004).

68. S. S. Alias, A. B. Ismail, and A. A. Mohamad, "Effect of pH on ZnO nanoparticle properties synthesized by sol-gel centrifugation." *J. Alloys Compd.*, **499**, 231 (2010).

69. R.,. N. T. Siswanto and P. Riski Akwalia, "Fabrication and characterization of zinc oxide (ZnO) nanoparticle by sol-gel method." *JPhCS*, **853**, 012041 (2017).

70. K. Lee, B. H. Guan, H. M. Zaid, H. Soleimani, and D. L. C. Ching, "Impact of pH on zinc oxide particle size by using sol-gel process." *In AIP Conference Proceedings*, **1787**, 050011 (2016), AIP Publishing LLC.

71. R. Ashraf, S. Riaz, S. S. Hussain, and S. Naseem, "Effect of pH on properties of ZnO nanoparticles." *Mater. Today Proc.*, **2**, 5754 (2015).

72. M. S. Akhtar, S. Riaz, R. Noor, and S. Naseem, "Optical and structural properties of ZnO thin films for solar cell applications." *Adv. Sci. Lett.*, **19**, 834 (2013).

73. S. Iwan, J. L. Zhao, S. T. Tan, and X. W. Sun, "Enhancement of UV photoluminescence in ZnO tubes grown by metal organic chemical vapour deposition (MOCVD)." *Vacuum*, **155**, 408 (2018).

74. R. S. Mohar, S. Iwan, D. Djuhana, C. Imawan, A. Harmoko, and V. Fauzia, "Post-annealing effect on optical absorbance of hydrothermally grown zinc oxide nanorods." *In AIP Conference Proceedings*, **1729**, 020024 (2016), AIP Publishing LLC.

75. S. T. Tan, B. J. Chen, X. W. Sun, X. Hu, X. H. Zhang, and S. J. Chua, "Properties of polycrystalline ZnO thin films by metal organic chemical vapor deposition." *J. Cryst. Growth*, **281**, 571 (2005).

76. I. Sugihartono, C. Retnoningtyas, C. Rustana, Umiatin, N.,. I. Yudasari, and F. Kurniadewi, "The influence of calcination temperature on optical properties of ZnO nanoparticles." *In AIP Conference Proceedings*, **2169**, 060010 (2019), AIP Publishing LLC.

77. K. Omri, I. Najeh, R. Dhahri, J. El Ghoul, and L. El Mir, "Effects of temperature on the optical and electrical properties of ZnO nanoparticles synthesized by sol-gel method." *Microelectron. Eng.*, **128**, 53 (2014).

78. Z. N. Kayani, F. Saleemi, and I. Batool, "Effect of calcination temperature on the properties of ZnO nanoparticles." *Appl. Phys. A*, **119**, 713 (2015).

79. Z. Z. Zhi, Y. C. Liu, B. S. Li, X. T. Zhang, Y. M. Lu, D. Z. Shen, and X. W. Fan, "Effects of thermal annealing on ZnO films grown by plasma enhanced chemical vapour deposition from Zn (C2H5) 2 and CO₂ gas mixtures." *J. Phys. D*, **36**, 719 (2003).

80. R. Ashraf, S. Riaz, Z. N. Kayani, and S. Naseem, "Effect of Calcination on properties of ZnO nanoparticles." *Mater. Today Proc.*, **2**, 5468 (2015).

81. A. Sangeetha, S. J. Seeli, K. P. Bhuvana, M. A. Kader, and S. K. Nayak, "Correlation between calcination temperature and optical parameter of zinc oxide (ZnO) nanoparticles." *J. Sol-Gel Sci. Technol.*, **91**, 261 (2019).

82. U. Manzoor, F. Tuz Zahra, S. Rafique, M. T. Moin, and M. Mujahid, "Effect of synthesis temperature, nucleation time, and postsynthesis heat treatment of ZnO nanoparticles and its sensing properties." *J. Nanomater.*, **2015** (2015).

83. C. Q. Sun, "Size and confinement effect on nanostructures." *ChemInform*, **37**, 1 (2006), arXiv preprint cond-mat/0506113.

84. D. Kim, K. D. Min, J. Lee, J. H. Park, and J. H. Chun, "Influences of surface capping on particle size and optical characteristics of ZnS: Cu nanocrystals." *Materials Science and Engineering: B*, **131**, 13 (2006).

85. T. M. Hammad, J. K. Salem, and R. G. Harrison, "Binding agent affect on the structural and optical properties of ZnO nanoparticles." *Rev. Adv. Mater. Sci*, **22**, 74 (2009).

86. W. L. Sin, K. H. Wong, and P. Li, "Surfactant effect on synthesis of nanocrystalline LaxSr1− xMnO₃ by hydrothermal method." *Acta Phys. Pol. A*, **111**, 165 (2007).

87. W. L. Tan and M. A. Bakar, "The effect of additives on the size of Fe₃O₄ particles." *J. Phys. Sci*, **17**, 37 (2006).

88. T. K. Kundu, N. Karak, P. Barik, and S. Saha, "Optical properties of ZnO nanoparticles prepared by chemical method using poly (vinyl alcohol)(PVA) as capping agent." *International Journal of Soft Computing and Engineering*, **1**, 19 (2011).

89. M. Thirumavalavan, K. L. Huang, and J. F. Lee, "Preparation and morphology studies of nano zinc oxide obtained using native and modified chitosans." *Materials*, **6**, 4198 (2013).

90. Y. L. Wu, A. I. Y. Tok, F. Y. C. Boey, X. T. Zeng, and X. H. Zhang, "Surface modification of ZnO nanocrystals." *Appl. Surf. Sci.*, **253**, 5473 (2007).

91. F. Bai, P. He, Z. Jia, X. Huang, and Y. He, "Size-controlled preparation of monodispersed ZnO nanorods." *Mater. Lett.*, **59**, 1687 (2005).

92. M. Guo, P. Diao, and S. Cai, "Hydrothermal growth of well-aligned ZnO nanorod arrays: Dependence of morphology and alignment ordering upon preparing conditions." *J. Solid State Chem.*, **178**, 1864 (2005).

93. P. Chandrasekaran, G. Viruthagiri, and N. Srinivasan, "The effect of various capping agents on the surface modifications of sol-gel synthesised ZnO nanoparticles." *J. Alloys Compd.*, **540**, 89 (2012).

94. M. Navaneethan, J. Archana, M. Arivanandhan, and Y. Hayakawa, "Chemical synthesis of ZnO hexagonal thin nanodisks and dye-sensitized solar cell performance." *Physica Status Solidi (RRL)–Rapid Research Letters*, **6**, 120 (2012).

95. G.,. N. Suman, N. Prabhakar, and R. Kumar, "Study of structural, optical and electrochemical properties of ZnO nanostructures and ZnO-PANI nanocomposites." *Mater. Res. Express*, **7**, 025024 (2020).

96. E. Rauwel, A. Galeckas, P. Rauwel, M. F. Sunding, and H. Fjellvåg, "Precursor-dependent blue-green photoluminescence emission of ZnO nanoparticles." *The Journal of Physical Chemistry C*, **115**, 25227 (2011).

97. S. Tachikawa, A. Noguchi, T. Tsuge, M. Hara, O. Odawara, and H. Wada, "Optical properties of ZnO nanoparticles capped with polymers." *Materials*, **4**, 1132 (2011).

98. M. R. Parra and F. Z. Haque, "Aqueous chemical route synthesis and the effect of calcination temperature on the structural and optical properties of ZnO nanoparticles." *Journal of Materials Research and Technology*, **3**, 363 (2014).

99. D. Verma, A. K. Kole, and P. Kumbhakar, "Red shift of the band-edge photoluminescence emission and effects of annealing and capping agent on structural and optical properties of ZnO nanoparticles." *J. Alloys Compd.*, **625**, 122 (2015).

100. A. Naveed Ul Haq, A. Nadhman, I. Ullah, G. Mustafa, M. Yasinzai, and I. Khan, "Synthesis approaches of zinc oxide nanoparticles: the dilemma of ecotoxicity." *J. Nanomater.*, **2017**, 8510342 (2017).

101. M. Nasrollahzadeh and S. M. Sajadi, "Green synthesis of copper nanoparticles using Ginkgo biloba L. Leaf extract and their catalytic activity for the Huisgen [3 + 2] cycloaddition of azides and alkynes at room temperature." *J. Colloid Interface Sci.*, **457**, 141 (2015).

102. X. Feng, Y. Yan, B. Wan, W. Li, D. P. Jaisi, L. Zheng, J. Zhang, and F. Liu, "Enhanced dissolution and transformation of ZnO nanoparticles: the role of inositol hexakisphosphate." *Environmental Science & Technology*, **50**, 5651 (2016).

103. M. Auffan, J. Rose, M. R. Wiesner, and J. Y. Bottero, "Chemical stability of metallic nanoparticles: a parameter controlling their potential cellular toxicity in vitro." *Environ. Pollut.*, **157**, 1127 (2009).

104. Z.-U.-R. Mashwani, M. A. Khan, T. Khan, and A. Nadhman, "Applications of plant terpenoids in the synthesis of colloidal silver nanoparticles." *Adv. Colloid Interface Sci.*, **234**, 132 (2016).

105. Z.-U.-R. Mashwani, T. Khan, M. A. Khan, and A. Nadhman, "Synthesis in plants and plant extracts of silver nanoparticles with potent antimicrobial properties: current status and future prospects." *Appl. Microbiol. Biotechnol.*, **99**, 9923 (2015).

106. T. Klaus-Joerger, R. Joerger, E. Olsson, and C. G. Granqvist, "Bacteria as workers in the living factory: metal-accumulating bacteria and their potential for materials science." *Trends Biotechnol.*, **19**, 15 (2001).

107. N. A. Samat and R. M. Nor, "Sol-gel synthesis of zinc oxide nanoparticles using Citrus aurantifolia extracts." *Ceram. Int.*, **39**, S545 (2013).

108. F. He, P. Yang, D. Wang, N. Niu, S. Gai, and X. Li, "Self-assembled β-NaGdF4 microcrystals: hydrothermal synthesis, morphology evolution, and luminescence properties." *Inorg. Chem.*, **50**, 4116 (2011).

109. C. L. Carnes and K. J. Klabunde, "Synthesis, isolation, and chemical reactivity studies of nanocrystalline zinc oxide." *Langmuir*, **16**, 3764 (2000).

110. M. N. Conde, K. Dakhsi, H. Zouihri, K. Abdelouahdi, L. Laanab, M. Benaissa, and B. Jaber, "Preparation of ZnO nanoparticles without any annealing and ripening treatment." *Journal of Materials Science and Engineering. A*, **1**, 985 (2011).

111. X. Guo, Q. Zhang, X. Ding, Q. Shen, C. Wu, L. Zhang, and H. Yang, "Synthesis and application of several sol–gel-derived materials via sol–gel process combining with other technologies: a review." *J. Sol-Gel Sci. Technol.*, **79**, 328 (2016).

112. Y. Z. Hao, Q. L. Zhang, J. Zhang, C. R. Xin, and H. Yang, "Enhanced sintering characteristics and microwave dielectric properties of Li 2 TiO 3 due to nano-size and nonstoichiometry effect." *J. Mater. Chem.*, **22**, 23885 (2012).

113. Q. L. Zhang, F. Wu, H. Yang, and D. Zou, "Preparation and dielectric properties of (Ca 0.61, Nd 0.26) TiO 3 nanoparticles by a sol–gel method." *J. Mater. Chem.*, **18**, 5339 (2008).

114. Q. L. Zhang, F. Wu, and H. Yang, "Sol–gel synthesis of A-site-ordered and homogeneous (Nd0. 55, Li0. 35) TiO3 ceramic and its dielectric properties." *Scr. Mater.*, **65**, 842 (2011).

115. Q. L. Zhang, H. Yang, and H. P. Wang, "Preparation of CuO-TiO $\sim$ 2 composite nanopowder and in situ doping in Al $\sim$ 2O $\sim$ 3 microwave dielectric ceramics." *JOURNAL-ZHEJIANG UNIVERSITY ENGINEERING SCIENCE*, **40**, 1450 (2006).

116. X. Guo, H. Yang, X. Zhu, Z. Lin, and L. Zhang, "Rheological properties and spray-drying behaviors of nano-SiC based aqueous slurry." *Mech. Mater.*, **46**, 11 (2012).

117. X. Guo, H. Yang, X. Zhu, and L. Zhang, "Preparation and properties of nano-SiC-based ceramic composites containing nano-TiN." *Scr. Mater.*, **68**, 281 (2013).